2015

Axon Initial Segment Stability in Multiple Sclerosis

Suneel K. Thummala
Virginia Commonwealth University

AXON INITIAL SEGMENT STABILITY IN MULTIPLE SCLEROSIS

A thesis submitted in partial fulfillment of the requirements for the degree of Master of Science at Virginia Commonwealth University.

by

SUNEEL KRISHNA THUMMALA
M.B.B.S, Vydehi Institute of Medical Sciences and Research Centre, 2012

Thesis Advisor: JEFFREY L. DUPREE, PH.D.
ASSOCIATE PROFESSOR
DEPARTMENT OF ANATOMY AND NEUROBIOLOGY

Virginia Commonwealth University
Richmond, Virginia
December, 2015

ACKNOWLEDGEMENT

I would like to express my gratitude to my advisor, Dr. Dupree, for his guidance and support. He is a truly exceptional mentor, who has played an integral role in my professional and personal development. I cannot overstate the value of his endless wisdom and patience, and commitment to my success. It was an honor to work in his lab and I feel truly privileged to have been a part of his research team.

I would also like to thank my committee members, Dr. Oh and Dr. Murthy, for their insight, patience and support at every step of the way from conception to fruition of this project. I would like to thank Dr. Henderson and the microscopy facility team for providing me essential guidance and training in research techniques.

I would like to extend my appreciation to my lab members, for their friendship and support. I would specifically like to thank my lab member Kareem Clark. He has been an incredible resource for knowledge and assistance at seemingly any time of the day, and has been indispensable to the success of my project.

Finally, I would like to thank my family for their unconditional love and support as I pursued my goals.

TABLE OF CONTENTS

LIST OF FIGURES

Page

LIST OF TABLES

Page

LIST OF ABBREVIATIONS

AIS	axon initial segment
ankG	ankyrinG
APP	amyloid precursor protein
BBB	blood brain barrier
BSA	bovine serum albumin
CIS	clinically isolated syndrome
CNP	2′:3′-Cyclic nucleotide-3′-phosphodiesterase
CNS	central nervous system
EAE	experimental autoimmune encephalomyelitis
FOV	field of view
GalC	galactosylceramide
HLA DR	human leukocyte antigen DR
HRP	horseradish peroxidase
IBA-1	ionized calcium binding adaptor molecule 1
INF-γ	interferon-γ
Kv	voltage gated potassium channel
MAG	myelin associated glycoprotein
MBP	myelin basic protein
MMP	metalloproteinases
MOG	myelin oligodendrocyte protein
MRI	magnetic resonance imaging

MS	multiple sclerosis
Nav	voltage gated sodium channel
NAWM	normal appearing white matter
Nfasc	neurofascin
NoR	node of Ranvier
OCT	optimal cutting temperature
PBS	phosphate buffered saline
PBST	phosphate buffered saline tween
PLP	proteolipid protein
PNS	peripheral nervous system
PPMS	primary progressive multiple sclerosis
PT	Pertussis toxin
RRMS	relapsing remitting multiple sclerosis
SDS	sodium dodecyl sulfate
SGalC	sulfogalactosylceramide
SPMS	secondary progressive multiple sclerosis
TNF-α	tumor necrosis factor-α

ABSTRACT

AXON INITIAL SEGMENT STABILITY IN MULTIPLE SCLEROSIS

By Suneel Krishna Thummala M.B.B.S.

A thesis submitted in partial fulfillment of the requirements for the degree of Master of Science at Virginia Commonwealth University.

Virginia Commonwealth University, 2015.

Thesis Advisor: Jeffrey L. Dupree, Ph.D.
Associate Professor of Anatomy and Neurobiology

Multiple sclerosis (MS) is an autoimmune disease of the central nervous system characterized by inflammation and demyelination. In addition to these hallmark features, MS also presents with axonal pathology, which is likely responsible for the signs and symptoms of the disease. Although prominent in MS, axonal pathology is frequently considered a consequence of demyelination and not a primary event. This conclusion is consistent with demyelination inducing the loss of specific axonal domains, known as the nodes of Ranvier that are responsible for the propagation of action potentials along the axon. In contrast, we propose that axonal pathology associated with MS is also independent of demyelination, and not a product of it. In support of our hypothesis, we have analyzed a different axonal domain known as the axon initial segment. Whereas a single axon has numerous nodes of Ranvier uniformly distributed along the axon, each axon contains only a single axon initial segment that is positioned immediately distal to the neuronal cell body. The axon initial segment is responsible for action potential generation and modulation, and

hence is essential for normal neuronal function. Background studies conducted by our lab, employing a murine model of demyelination/remyelination, revealed no correlation between axon initial segment stability and myelin integrity. Here we investigate the fate of the axon initial segment in human multiple sclerosis. While not statistically significant, we provide data demonstrating an apparent 40% reduction in AIS numbers in MS. These findings are, however, highly preliminary due to the limited number of samples. We further provide qualitative evidence that AIS disruption in MS is not dependent on demyelination suggestive that axonal pathology may be a primary event in MS. Our current findings are intriguing, but unfortunately this study is underpowered, and more samples will be required to determine whether this apparent reduction is statistically significant.

INTRODUCTION

Multiple sclerosis is a pervasive, debilitating disease of the central nervous system. In the early 19th century, Charcot first described the 'sclerotic plaques' from which the disease eventually got its name (Charcot, 1868; as reviewed in Kornek and Lassmann, 1999). These plaques are the histopathological hallmark feature of this prototype demyelinating disease, characterized by the presence of well circumscribed, multifocal inflammatory demyelinated lesions distributed over time and space within the CNS (Files, 2015; Haines, 2012; Grigoriadisa, 2004). MS affects approximately 400,000 individuals in the United States and affects 2.5 million individuals worldwide (World Health Organization, 2008). Despite being clinically silent for a large portion of its process, MS eventually presents with non-specific cognitive symptoms such as sensory disturbances, ophthalmoplegia, parasthesias, neuralgias, ataxia and/or neurogenic bowel and bladder symptoms (Noseworthy, 2000; Files, 2015). As the disease advances, patients undergo progressive cognitive and/or psychiatric decline, having life expectancies shortened by 5-10 years, attributable to increased risk of complications from neurological disability (Compston and Coles, 2008). While studies have demonstrated a strong correlation between this progressive neurological impairment and neurodegenerative pathology, this process is traditionally considered to be a consequence of demyelination (Hauser and Oksenberg, 2006). It has recently been proposed that axonal pathology in MS could be a primary event in the disease process (Trapp et al., 1998; Trapp and Nave, 2008; Haines et al., 2011). This project aims to explore this

concept, specifically investigating the susceptibility of a particular axonal domain, the axon initial segment (AIS) to the multiple sclerosis disease process.

The Neuron:

Neurons are the specialized cell types of the central and peripheral nervous systems. They are polarized cells, responsible for intercellular communication through electrical or chemical signaling within the nervous system and to target organs. Neurons are structurally and functionally composed of 3 distinct parts: the dendrites, the cell body and the axon. Together the dendrites and the cell body constitute the somatodendritic region. Dendrites are short membranous processes exhibiting a tapered morphology, responsible for the reception and integration of electrical and/or chemical synaptic inputs from neurons and other cells (Kevenaar and Hoogenrad, 2015). The axon is the thin, long projection from the neuronal cell body that transmits the signal to the receptors of subsequent neurons or other cells, in the form of an electrical wave called the action potential (Stiess and Bradke, 2011). The axon is composed of specialized regions, such as: the axon hillock, axon initial segment, nodes of Ranvier and the axon terminal, each playing a vital role in this process. The axon hillock bridges the soma and the axon, and is the site where inhibitory and excitatory synaptic inputs summate. The region adjacent to the axon hillock is the axon initial segment, a highly specialized domain, composed unique structural proteins and ion channels that allow for the generation and modulation of an action potential (Clark et al., 2009; Buffington and Rasband, 2011). The nodes

Figure 1. Schematic representation of a neuron. The chief components of a typical CNS neuron highlighting the cell body (soma) and the axon, and their various subparts. An oligodendrocyte and its contributing myelin sheath are also observable. The axonal domains, the nodes of Ranvier and the axon initial segment are labelled.

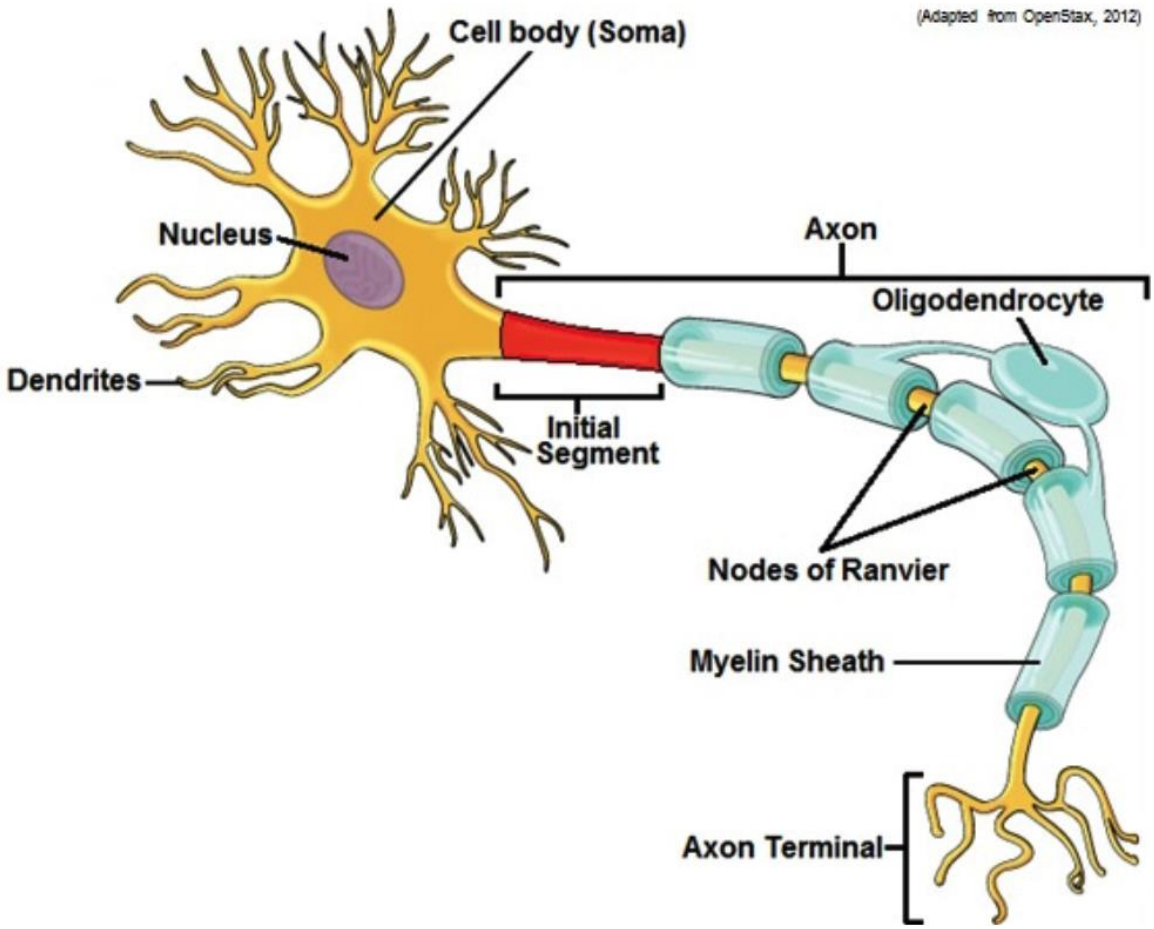
(Adapted from OpenStax, 2012)
Cell body (Soma)
Nucleus
Axon
Oligodendrocyte
Dendrites
Initial Segment
Nodes of Ranvier
Myelin Sheath
Axon Terminal

Figure 1

of Ranvier (NoR) are short regions of the axon that lack a myelin sheath (the insulating membrane that wraps around the axon). Both the myelin sheath as well as the NoRs function in action potential propagation along the axon, ending in the axon terminal, where the impulse is transmitted to target cells/organs through the synapse, via electrical or chemical signals (Susuki and Rasband, 2008)

Myelin:

The term 'myelin', first coined by Rudolf Virchow in 1864, is used to describe the lipid dense extension of the plasma membrane of oligodendrocytes (in the CNS) and Schwann cells (in the PNS), which surrounds the axon, forming an insulating sheath (Raine, 1984; Snaidero and Simons, 2014; Boulanger and Messier, 2014; Alizadeh et al., 2015). By insulating the axon, and clustering sodium channels into the nodes of Ranvier, myelin reduces the transverse capacitance and increases the transverse resistance of the axonal plasma membrane, crucial for saltatory nerve conduction, the basis of rapid information processing and communication between networks of nerve cells in the CNS (Aggarwal et al., 2011; Nave and Werner., 2014; Hartline and Colman, 2007). Oligodendrocytes, the myelin-forming cells of the CNS, extend their plasma membranes in concentric loops, each process contacting and enveloping a segment of the axon, forming a multi-layered sheath (Tomassy et al., 2015). In addition to myelin generation, oligodendrocytes secrete metabolic factors that are essential for the survival and integrity of CNS neurons (Tomassy et al., 2015; Chamberlain et al., 2015; Edgar et al., 2009; Fünfschilling et al., 2012; Lee et al.,

2012; Oluich et al., 2012). Maintenance and repair of the myelin sheath occurs throughout adult life and includes spontaneous remyelination of neurons by oligodendrocytes and their precursors (Irvine and Blakemore, 2008; Jeffery and Blakemore, 1997; Kornek et al., 2000).

With an unusually high lipid concentration compared to other biological membranes, myelin is composed of 30% protein and 70% lipid, a configuration that is essential to myelin's insulating property and function (Aggarwal et al., 2011) The abundance of cholesterol, which constitutes 24-28% of total myelin lipids, likely restricts membrane fluidity and carving affecting intercellular trafficking (Jahn et al., 2009). Cholesterol is also the rate-limiting step in the formation of myelin, as demonstrated by experiments conducted using Zebrafish, lacking the enzyme for cholesterol synthesis (Mathews et al. 2014; Saher et al. 2005, 2009) Other lipids of note are galactolipids, galactosylceramide (GalC), its sulfated form 3-O-sulfogalactosylceramide (SGalC), and their hydroxylated forms GalC-OH and SGalC-OH, which together add up to 20–26% of total myelin lipids (Bosio et al., 1998). These lipids play crucial roles in interactions between the oligodendrocyte and the axon, as well as maintenance of myelination (Coetzee et al., 1996; Dupree et at., 1998; Bosio et al., 1998). Plasmalogens are a class of phospholipids that make up 12-15% of the total myelin lipid. Plasmalogens have an anti-oxidant effect, and decreased levels have been implicated in demyelination in X-linked adrenoleukodystrophy (Khan et al., 2008).

Of the principal protein components of CNS myelin, proteolipid protein (PLP) and its smaller splice isoform, DM20, are the most prominent, making up 30-45% of

myelin protein. PLP plays a role in the formation of the intraperiod line, however, despite their abundance, these proteins do not appear to play a vital role in the establishment or maintenance of myelin, as studies using PLP/DM20 knockout mice revealed periodicity issues, but did not show wide spread demyelination (Klugmann et al., 1997; Coetzee et al., 1999)

Myelin basic protein (MBP) is the second most abundant myelin protein, comprising up to 22–35% of total myelin protein. MBP plays a crucial role in myelin compaction and stabilizing the major dense line, and absence of MBP results in severe hypomyelination, as seen in the mouse mutant *shiverer* and the rat mutant *long evans shaker* (Roach et al., 1985; O'Connor et al., 1999).

Other proteins of interest include 2′:3′-Cyclic nucleotide-3′-phosphodiesterase (CNP), myelin-associated glycoprotein (MAG) and myelin-oligodendrocyte protein (MOG). CNP is a major component of non-compact myelin, and is associated with oligodendrocyte processes and paranodal loops and is said to play a role in the cytoskeletal network of myelin (DeAngelis and Braun, 1996). MAG functions in facilitating adhesion and signaling, between oligodendrocytes and axons, during myelin formation (Quarles et al., 1992; Quarles and Morell, 1999). MOG functions in transmitting extracellular information to the interior of oligodendrocytes (Quarles et al., 2006). It is of particular interest to us because it is the antigen that, when injected into an animal, elicits a cellular immune response that produces the CNS autoimmune disease experimental autoimmune encephalomyelitis (EAE).

Axonal Domains:

Myelinated axons show a high degree of structural and functional organization, and can be separated into several distinct, specialized domains; the node of Ranvier (NoR), the paranode, the juxtaparanode, the internode and the axon initial segment (AIS). These domains have similarities and differences with regards to structural protein composition, function, and mechanisms of establishment and maintenance. While they each play important roles in proper neuronal functioning, for the purposes of this thesis, we will focus on the node of Ranvier and the axon initial segment.

Nodes of Ranvier:

The nodes of Ranvier are myelin-bare regions of the axon spanning approximately 1- 2 μm in length (Peters et al., 1991; Salzer, 1997). The constricted diameter of the node of Ranvier results in slowed axonal transport and therefore, higher densities of vesicles, microtubules, mitochondria, and tightly packed neurofilaments (Fabricius et al., 1993; Peters et al., 1991; Salzer, 1997). Vital for its role in action potential propagation, the node contains a high concentration of voltage gated sodium channels (Nav), including isotypes; Nav 1.1, Nav 1.2 and Nav 1.6 (Arancibia‐Carcamo and Attwell, 2014; Buttermore et al., 2013; Thaxton and Bhat, 2009; Salzer, 1997). These sodium channels are anchored to the cytoskeleton through interaction, at either its α- or β- subunits, with the scaffolding protein ankyrinG (ankG) (Bennett and Lambert, 1999; Buttermore et al., 2013; Thaxton and Bhat, 2009). AnkG associates with the spectrin- actin cytoskeleton through interactions with βIV-

spectrin, which is exclusively localized in the node and axon initial segment (Berghs et al. 2000; Buttermore et al., 2013; Komada and Soriano, 2002). The node of Ranvier also contains extracellular matrix molecules, cell adhesion molecules and certain types of potassium channels.

Saltatory conduction is the process by which action potentials 'jump' across unexcitable portions of the axon (myelin segments) from one node to the next. This process is made possible by the high density clustering of sodium channels at the nodes of Ranvier where ion flow occurs exclusively after the impulse has left the AIS (Salzer, 2003; Sherman and Brophy, 2005). Ion channel clustering, as well as its interactions with the ankyrinG and βIV-spectrin/actin network, at the node of Ranvier is, therefore, vital for efficient action potential transmission (Bennett and Lambert, 1999; Buttermore et al., 2013; Thaxton and Bhat, 2009). AnkyrinG, described as the master regulator of AIS and NoR assembly (He et al., 2013; Kordeli et al., 1995; Jenkins and Bennett, 2001; Sobotzik et al., 2009; Hedstrom et al., 2008; Dzhashiashvili et al., 2007; Zhou et al. 1998), is responsible for the clustering of Nav channels at the NoR. Sodium channels are anchored to the actin-cytoskeleton through direct interaction with the scaffolding protein ankyrinG and indirect interaction through adapter protein βIV-spectrin (Rasband, 2010; Eshed-Eisenbach and Peles, 2013). Establishment of these interactions is critical for nodal clustering, as mice lacking these stabilizing cytoskeletal associated proteins (ankG and/or βIV-spectrin) display severely reduced sodium channel density (Gasser et al., 2012; Komada and Soriano, 2002; Yang et al., 2004). Additionally, not only is ankyrinG required for the establishment of the node of Ranvier, but it is also critical for

maintaining the nodal protein complexes; as knock down of ankG results in cluster dismantling (Hedstrom et al., 2008).

While myelin contact at the paranode is required for node of Ranvier formation it is also vital for nodal maintenance. Studies conducted by our lab and others show that compromised myelin-axon interactions result in a disruption of nodal protein domain organization (Eshed-Eisenbach and Peles, 2013; Susuki et al., 2013; Dupree et al., 1999). The Cuprizone model (discussed in detail later) is a demyelinating murine model, in which myelin-forming oligodendrocytes are killed, resulting in a complete loss of both nodally clustered sodium channels, as well as paranodal clusters of caspr (Dupree et al., 2004).

Axon Initial Segment:

The axon initial segment (AIS) is an unmyelinated region of the axon, spanning about 35-45 μm distally from the soma, located between the axon hillock and the first myelin segment, in myelinated neurons. (Bender and Trussell, 2012; Grubb and Burone, 2010; Rasband, 2010). The AIS serves as the site for action potential initiation and modulation, as well as a gatekeeper between the somatodendritic and axonal domains (Meeks et al., 2007; Rasband, 2010). Because the AIS and the node of Ranvier both play roles in action potential transmission, their protein clusters are very similar in composition (Rasband, 2010).

The axon initial segment serves as the action potential trigger zone due to its high density of voltage-gated sodium channels. The AIS integrates signals from the somatodendritic region of the neuron, and acts as an action potential threshold

"decision maker" (Inan et al., 2013; Kole and Stuart, 2012; Tai et al., 2014; Yosihmura and Rasband, 2014). Action potential amplitude, duration and frequency are thought to be regulated by the diversity of potassium channel subtypes (Kv1.2, Kv2.2 and Kv7.2) present in the AIS (Kole et al., 2007; Sánchez-Ponce et al., 2012). The AIS also undergoes frequent plasticity, such as changes in ion channel localization and expression, alterations in AIS length, and physical relocation of the AIS; all due, in part to synaptic input and pruning; thus fine-tuning neuronal excitability (Adachi et al., 2014; Grubb and Burrone; Kaphzan et al., 2011; Kuba et al., 2010,2012).

In addition to its role in action potential initiation and modulation, the axon initial segment serves as a barrier between the somatodendritic and axonal domains; thus maintaining neuronal polarity (Rasband, 2010). The mechanism underlying this barrier is not fully understood, but it is hypothesized that the vast number of AIS proteins could act as a sieve to weed out larger cytoplasmic molecules (Nakada et al., 2003; Rasband, 2010).

The axon initial segment, like the node, contains a high density of voltage gated sodium channels (Nav 1.1, Nav 1.2 and Nav 1.6); about 40-50 times that of the somatodendritic domains (Rasband, 2010; Kole et al., 2008). Unlike the node, which assists in the propagation of action potentials, these AIS Na+ channel clusters serve as the trigger zone (Meeks et al., 2007). Similar to the node, the AIS is composed of a variety of ion channels, cell adhesion molecules, extracellular matrix molecules and cytoskeletal scaffolds. The master organizer molecule ankyrinG is responsible for the interaction of these sodium channels to the axonal cytoskeleton and

Figure 2. Axon initial segment and its constituent proteins. Ion channels, cell adhesion molecules, neurotransmitter receptors and cytoskeletal proteins are enriched at the AIS. AnkyrinG, dubbed the 'master organizer' of the AIS binds β4 spectrin and Nav channels.

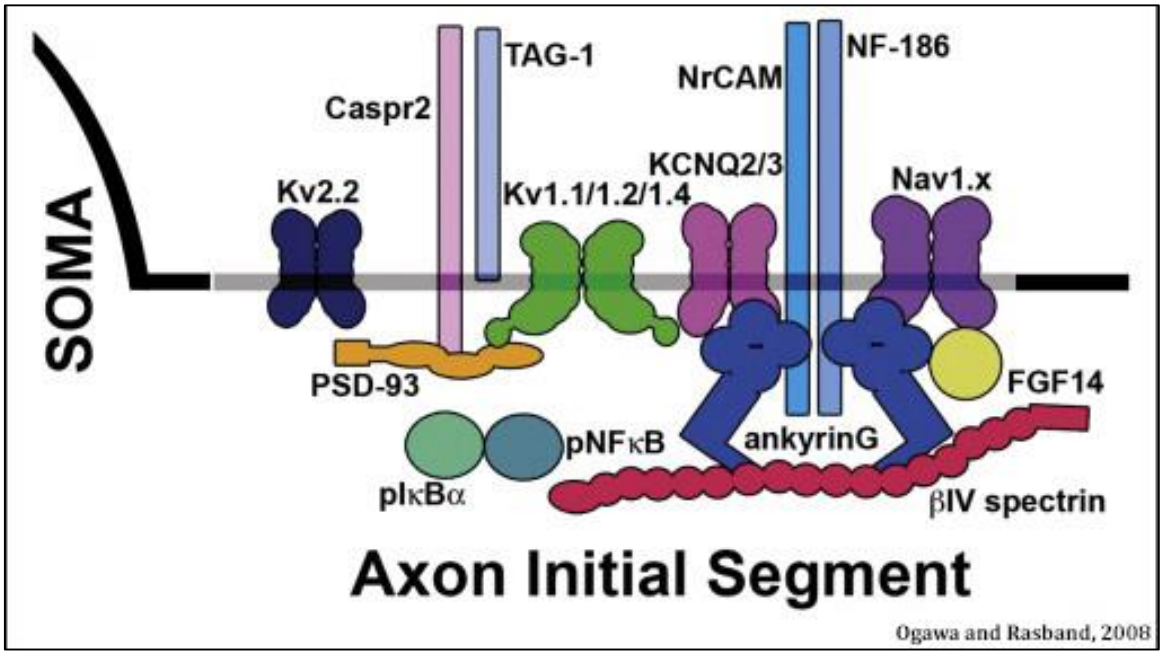
SOMA
TAG-1
Caspr2
NrCAM
NF-186
KCNQ2/3
Kv2.2
Kv1.1/1.2/1.4
Nav1.x
PSD-93
FGF14
pNFκB
ankyrinG
pIκBα
βIV spectrin
Axon Initial Segment
Ogawa and Rasband, 2008

Figure 2

maintenance of neuronal polarity. Additionally, ankG silencing and its removal from the mature AIS results in dismantling of the AIS, as detected through dispersion of sodium channel, βIV-spectrin, NF-186, and NrCAM immunolabeling (Hedstrom et al., 2008). AnkG is therefore, not only required for the initial recruitment and clustering of AIS proteins, but also for the long-term maintenance of this domain. Recently, the first human mutations in ankG were reported and shown to be associated with severe intellectual disability, attention deficit hyperactivity disorder, and autism (Iqbal et al., 2013).

Although the node of Ranvier and the AIS contain very similar protein clusters, they are established and maintained through different processes, the most noteworthy being their relationship with myelin. While both the formation and maintenance of the node of Ranvier requires myelin contact, the AIS is formed intrinsically through ankG restriction to the proximal end of the developing axon, completely independent of myelination (Bennett and Baines, 2001; Galiano et al., 2012). Data regarding the maintenance of the AIS with relation to myelin, is however limited. Preliminary studies show that myelin may not be required to preserve AIS integrity (Clark et al., [in review]; Hamada and Kole, 2015).

Multiple Sclerosis:

Multiple sclerosis (MS) is a debilitating neurological disease, characterized by the immune mediated destruction of the myelin sheath, with subsequent neurological

damage (Compston and Coles, 2002). MS is the leading cause of neurological disability in young adults, and currently affects over 400,000 people in the United States, and over 2.5 million people worldwide (Hauser and Oksenberg, 2006; Noseworthy, 1999; Noseworthy et al., 2000; Trapp and Nave, 2008; Weinshenker, 1998). MS shows a peculiar worldwide distribution, with increased prevalence in populations progressively further away from the equator. MS also disproportionately affects females more than males, at a ratio of ~3:1 (Ahlgren *et al.* 2011; Compston and Coles, 2002; Orton *et al.* 2010; Wallin *et al.* 2012). MS is a highly variable disease, believed to arise from a combination of genetic interactions and environmental influences, but little is truly known about its cause or the factors contributing to its unpredictable course and outcome (Compston and Coles, 2008) Multiple sclerosis may follow one of four clinical courses based on disease activity and progression: clinically isolated syndrome (CIS), relapsing-remitting multiple sclerosis (RRMS), primary progressive multiple sclerosis (PPMS), and secondary progressive multiple sclerosis (SPMS) (Lublin et al., 2014).

Clinically isolated syndrome (CIS) presents as a single isolated attack, characterized by symptoms compatible with MS, but has yet to fulfill MS diagnostic criteria. These patients may or may not progress to full blown MS (Miller et al., 2012). Approximately 85 to 90 percent of affected adults develop relapsing-remitting multiple sclerosis (RRMS) at onset, with a clinical course characterized by intermittent attacks of increased disability followed by either partial or complete recovery to their baseline function (Simone et al., 2002; Gusev et al., 2002; Banwell et al., 2007; Renoux et al., 2007; Boiko et al., 2002). RRMS may evolve to secondary

progressive multiple sclerosis (SPMS) in individuals who eventually show progressive neurological decline without acute attacks or periods of remission. Primary progressive multiple sclerosis (PPMS), a disease type characterized by continuous disability over time in the absence of specific attacks, is much less common than RRMS. A PPMS course is associated with the most rapid disease progression and has the poorest prognostic value (Weinshenker, 1994; Tremlett et at., 2006).

Pathogenesis:

Multiple sclerosis is thought to be attributable to an autoreactive attack on myelin and oligodendrocytes by cells of the immune system that have entered the brain and/or spinal cord, manifesting as acute focal inflammatory demyelination and axonal loss with limited remyelination, culminating in the chronic multifocal sclerotic plaques from which the disease gets its name. (Trapp and Nave, 2008) To better understand the characteristic pathology of MS, we will tease apart and examine each aspect individually.

MS Inflammation:

Inflammation in MS is believed to be mediated by a coordinated attack by T lymphocytes and macrophages, against CNS tissue (Boppana et al., 2011). T cells cross the blood brain barrier to enter the CNS. Activation of autoimmune responses against myelin components in the CNS is hypothesized to occur through a variety of

mechanisms such as molecular mimicry, bystander activation and epitope spreading (Trapp and Nave, 2008; Popescu and Lucchinetti, 2012; Vanderlugt and Miller, 2002; von Herrath et al., 2003). As lymphocytes secrete matrix metalloproteinases (MMP) to break down the blood brain barrier (BBB), the activated, autoreactive T lymphocytes in the periphery, attach themselves to the receptors of endothelial cells, granting them access through the BBB and into the central nervous system (Compston and Coles, 2002, Hauser and Oksenberg, 2006). Once inside CNS parenchyma, the T cells, reactivated by CNS myelin, stimulate pro-inflammatory cytokines, such as TNF- α (Peterson and Fujinami, 2007; Hauser and Oksenberg, 2006), which stimulate the resident microglia and recruit B cells, astrocytes and macrophages. Microglia secrete a host of factors such as TNFα (Haji et al., 2012), iNOS (Starossom et al., 2012), IL-1β, COX2 and generate reactive oxygen species (Guemez-Gamboa et al., 2011; Block et al., 2007) setting up a pro-inflammatory loop. This combination of events creates an environment in which the hallmark pathological processes of multiple sclerosis: demyelination and neuronal damage, occur.

MS Demyelination:

The pathologic hallmark of MS consists of areas of focal demyelination, known as plaques, characterized by reactive glial scar formation, inflammation, and partial axonal sparing (Kutzelnigg and Lassmann, 2014). Both humoral and cell mediated immune mechanisms play roles in the formation of these demyelinated lesions. As described earlier, autoreactive T cells are responsible for the propagation of a highly

inflammatory environment, bind to MHC class I antigens on oligodendrocytes to cause cell injury or they may produce demyelination through the endogenous production of inflammatory cytokines, such as tumor necrosis factor-α (TNF-α) and interferon-γ (INF-γ) (Noseworthy, 1999). Additionally, T cells drive the activation and recruitment of microglia and macrophages, both key players in the initial and sustained immune response to myelin antigens. Apart from secreting a variety of cytotoxic and inflammatory factors, microglia can directly contact the myelin sheath and oligodendrocytes, delivering lethal signals through surface bound TNFα (Zajicek et al., 1992; Compston and Coles, 2002).

B cell activation and production of antibodies play a critical role in the development of demyelination. Antibodies to myelin antigens such as myelin basic protein (MBP) and myelin oligodendrocyte protein (MOG) have been detected in MS plaques (Genain et al., 1999; O'Connor et al., 2005; O'Connor et al., 2007). Studies show that novel targets to non-myelin antigens such as KIR4.1, neurofascin and SPAG-16 mediate demyelination and axonal disruption (Fraussen et al., 2014; Levin et al., 2013).

Demyelinated plaques in MS can be observed in both the white matter, as well as cortical and subcortical gray matter (Brück 2005; Calabrese 2015). Plaques are graded based on macrophage activity within the lesion. Acute active plaques are characterized by massive infiltration of myelin-laden macrophages, with relative axonal preservation and variable loss of oligodendrocytes (Brück et al., 1995; Kutzelnigg and Lassmann, 2014; Popescu and Lucchinetti, 2012). Other demyelinated lesions of interest are, chronic active plaques: regions of peripheral

macrophage activity with hypocellular, gliotic centers; inactive plaques: completely demyelinated, hypocellular lesions; and shadow plaques: sharply circumscribed, light myelin staining regions representing areas of partial remyelination (Popescu and Lucchinetti, 2012; Sobel and Moore, 2008; Prineas et al., 2001; Lucchinetti and Bruck, 2004).

MS Neurodegeneration:

While multiple sclerosis has historically been considered a prototype demyelinating disease, neuronal pathology plays an integral role in the functional pathogenesis of MS. Charcot's findings, describing substantial axonal damage in active lesions (Kornek and Lassmann, 1999), were largely ignored until more recent landmark papers revealed abundant transected and dystrophic axons in sites of active inflammation and demyelination, and confirmed that partial or total axonal transection begins early in the disease process (Bitsch et al., 2000, Ferguson et al., 1997 and Trapp et al., 1998). Various pathological studies have demonstrated reduced axonal density and in active, chronic and inactive plaques (DeLuca et al., 2004; Bjartmar et al., 2000; Bitsch et al., 2000; Frischer et al., 2009). Accumulation of amyloid precursor protein (APP) within the axon is caused by disruption of APP transport down the axon, and is evidence of compromised axonal structure integrity. APP accumulations have been observed in MS, within active lesions and chronic plaques (Lovas et al., 2000; Mews et al., 1998; Ferguson et al., 1997). Axonal pathology is further evidenced by magnetic resonance imaging (MRI) techniques, visualizing whole brain atrophy (Miller et al., 2002), worsening focal (T1) lesions

(Bagnato et al., 2003), disruption of white matter tracts, and altered functional connectivity by functional MRI (Cader et al., 2006).

The mechanisms driving neuronal pathology in MS are of particular importance, as there appears to be a correlation between cumulative axonal loss and progressive, irreversible neurological disability (Neumann, 2003; Matthews et al., 1998; Paolillo et al., 2000; Fisher et al., 2000; Grimaud et al., 1999). As with demyelination, neuroaxonal damage in MS is a multifactorial process.

We are yet to fully understand the mechanisms driving axonal pathology in MS. A correlation between demyelination and axonal loss has been demonstrated by numerous studies. Progressive axonal degeneration and disability was observed in murine models lacking either myelin associated glycoprotein (MAG) or proteolipid protein (PLP) (Li et al., 1994; Griffiths et al., 1998). Similar findings were observed in humans carrying a null mutation in the gene encoding PLP1 (Garbern et al., 2002). Histopathology of post mortem human MS tissue has shown axonal transections in lesions of active inflammation (Kornek et al., 2000; Trapp et al., 1998). Furthermore we know that the establishment and maintenance of axonal domains is dependent on myelination (Dupree et al., 1999; Dupree et al., 2004; Marcus et al., 2006; Pomicter et al., 2010).

The hypothesis that axonal damage in MS may occur independently of demyelination has been suggested by several studies and is a focus of this project. Axon-specific antibodies have been implicated in axonal degeneration (Zhang et al., 2005). Axonal damage has also been linked to the presence of reactive resident microglia, invading inflammatory immune cells, and their toxic metabolites. Release

of reactive oxygen species, specifically NO, by immune cells has been demonstrated to directly damage axons and mediate the development of neurological symptoms (Acar et al., 2003 and Smith, 2005). Studies using post mortem cortical tissue in MS patients, described axonal abnormalities in areas devoid of demyelination, termed normal appearing white matter (NAWM) (Siffrin et al., 2010; Ramió-Torrentà et al., 2006; De Stefano et al., 2003; Davies et al., 2004). The marked reduction of the neuron-specific marker N-acetyl aspartic acid in MS lesions, and normal appearing white matter (NAWM) in MS patients suggests that neuronal pathology can occur early in disease and prior to the formation of overt lesions (Siffrin et al., 2010). MRI studies on progressive brain atrophy have yet to prove that neuronal damage is secondary to demyelination (Rudick, et al., 1999; Miller et al., 2002; Narayan et al., 1997). Siffrin et al., in 2010, showed that cortical demyelination occurred in the late stages of the disease, and believed it to be a consequence rather than a cause, of neuronal loss (Siffrin et al., 2010). Thus axonal destabilization and damage has been shown to occur even in the absence of morphological evidence of demyelination, however, the mechanisms underlying this process as to how or where this damage precisely occurs, are still not entirely clear. We believe that investigating the stability of axonal domains, specifically the axon initial segment, could provide insight into the mechanisms regulating axonal degeneration and its relationship to myelination, in multiple sclerosis.

Background Data:

As more and more studies are establishing that axonal pathology independent of myelin loss is a viable explanation of the pathogenesis of multiple sclerosis, our lab decided to investigate the behavior of the axonal domain, the axon initial segment (AIS), under similar circumstances. To first address this, we employed murine models of multiple sclerosis.

EAE model:

To evaluate AIS integrity in an inflammatory environment, we utilized the murine model of chronic experimental autoimmune encephalomyelitis (EAE) as previously described (DeVries et al., 2012; Secor McVoy et al., 2015; Dupree et al., 2015). EAE is a murine model, which shares the inflammatory features of MS but none of the demyelinating aspects. 12 week old mice were injected with a cocktail consisting of myelin oligodendrocyte protein (MOG), Freund's adjuvant containing heat-killed M. tuberculosis and Pertussis toxin (PT). This induced an inflammatory CNS response, producing clinical symptoms as early as 5 days post-induction. Clinical motor symptoms were scored daily following immunization and were recorded as follows: 0= no signs, 1.0= limp tail, 2.0= loss of righting reflex, 3.0= paralysis of single hind limb and 4.0= paralysis of both hind limbs. Mice achieved peak clinical symptoms at ~15 days post induction. Two experimental time points were established: an early inflammatory time point (3 days post peak clinical symptoms) and a late inflammatory time point (9 days post peak clinical symptoms). Not all mice achieved maximum clinical scores by day 10, allowing us to exploit this variation to

investigate the correlation between disease severity and extent of axonal pathology. Within each time point, mice were categorized as either EAE 1&2, or EAE 3&4 based on clinical scoring.

Axon initial segments were shortened following early EAE:

Immunolabeling for markers directed against ankyrinG allowed visualization of axon initial segments (AIS) in cortical layer V of mice. Quantitative analysis of AIS numbers and length in layer V or the cortex of EAE mice at the early inflammatory time point revealed no change in AIS numbers among any of the groups. No change in AIS length was observed between naïve and early EAE 1&2, however early EAE 3&4 mice showed significantly shortened mean AIS lengths, compared to both the naïve and EAE 1&2 groups. To determine whether this shortening was an early event in progressive AIS disruption, or whether the shortening would spontaneously correct itself with disease progression, we quantified AIS numbers and lengths at the late inflammatory EAE time point.

Axon initial segments were lost during late EAE:

AIS morphology was assessed following 9 days post peak clinical symptoms (late EAE). In contrast to the mice at early EAE, quantification of AISs at the late EAE stage revealed significantly reduced numbers of AIS in both EAE 1&2 and EAE 3&4 groups compared to the naïve mice. As seen in Figure 3 approximately 60% of AISs

Figure 3. AIS length is reduced in early stages of EAE while the number of AISs is decreased in the late stages of disease. In Early disease stage (3 days post peak clinical symptoms), AISs in cortical layer V neurons of naïve (A) and EAE 1&2 (B) mice were abundant, presented with uniform length and rarely revealed discontinuous labeling indicative of fragmentation (yellow arrows). In contrast, AISs of layer V cortical neurons in Early EAE 3&4 mice (C) were frequently reduced in length (white arrows) and fragmented (yellow arrows). Quantitative analysis confirmed the immunohistochemical observations. No difference in AIS number was observed among the Early EAE groups (G). Although no difference in AIS length was observed between naïve and Early EAE 1&2 mice (H), a significant shortening was observed with the Early EAE 3&4 mice compared to naïve animals (H). In contrast, the Late EAE 1&2 mice (E,G) exhibited a significantly reduced in the number of AISs with a continued progression in AIS loss observed in the Late EAE 3&4 mice (F,G). While there was a significant decrease in AIS length for the Late EAE 1&2 mice, a significant but less dramatic shortening was observed for the Late EAE 3&4 mice as compared to the naïve animals (H). Note that with the loss of AISs (Panel F), punctate AnkG labeling was prevalent. Double labeling for AnkG and the paranodal marker caspr (see F inset; AnkG – red; caspr – green) revealed that these pucta were nodes of Ranvier that were not disrupted following EAE induction. (Asterisks with no associated bracket represent a significant difference from the naïve group; *p=0.0001, **p=0.008).

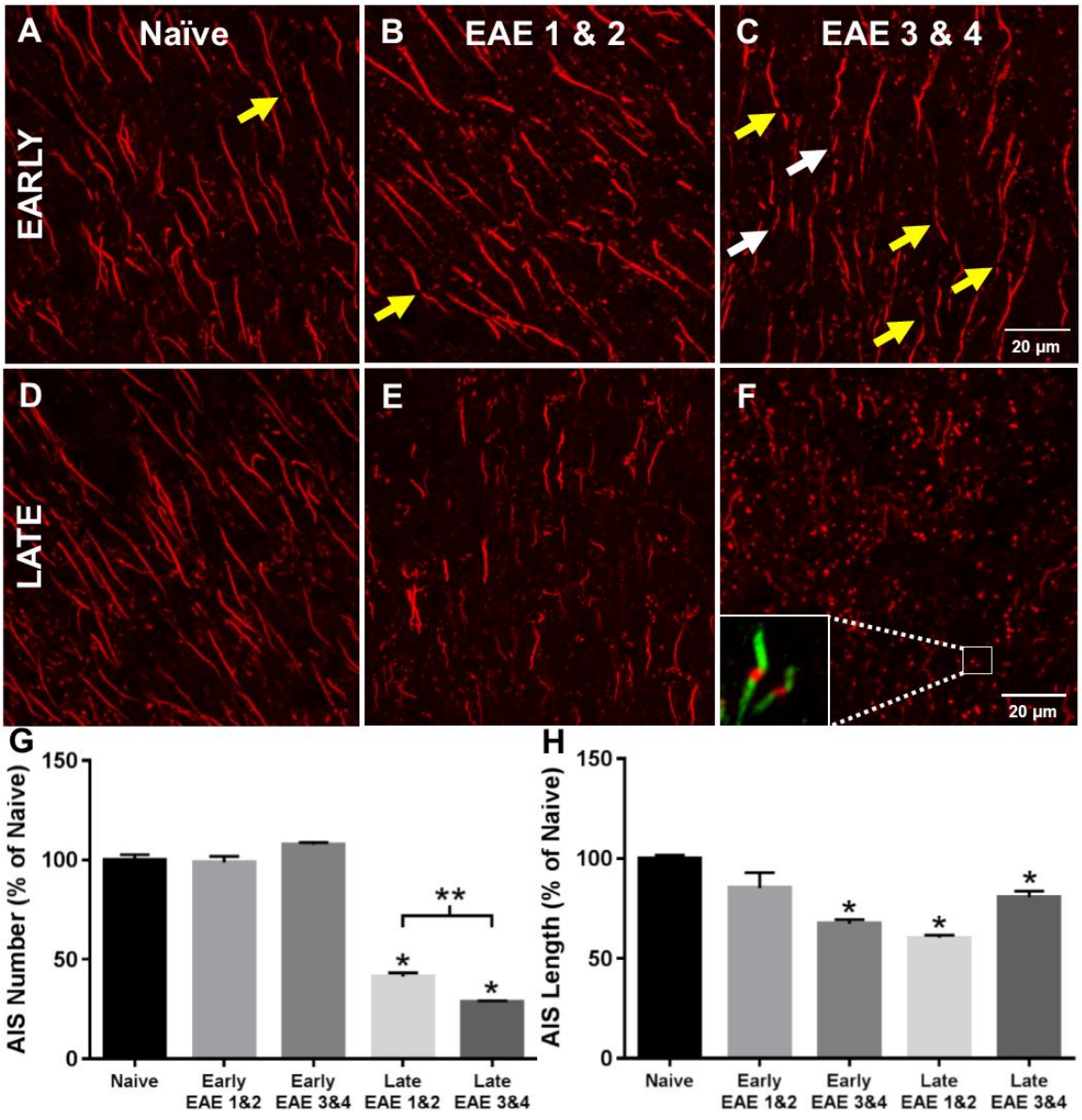
A
Naïve
B
EAE 1 & 2
C
EAE 3 & 4
EARLY
20 µm
D
E
F
LATE
20 µm
G
AIS Number (% of Naive)
150
100
50
0
**
*
*
Naive
Early EAE 1&2
Early EAE 3&4
Late EAE 1&2
Late EAE 3&4
H
AIS Length (% of Naive)
150
100
50
0
*
*
*
Naive
Early EAE 1&2
Early EAE 3&4
Late EAE 1&2
Late EAE 3&4

Figure 3

were lost in the late EAE 1&2 while nearly 75% of AISs were lost in the late EAE 3&4 mice. AIS lengths were measured at the late inflammatory time point as well, revealing significantly shorter AIS lengths in both EAE 1&2 and EAE 3&4 groups compared to the naïve mice.

Therefore, we show that the AIS are significantly shortened and the number significantly reduced in EAE mice. These findings are extremely exciting as they show a disruption of axonal protein domain organization in the absence demyelination.

Cuprizone Model:

Demyelination does not disrupt molecular organization of the AIS:

Although MBP labeling detected no demyelination in the cortex of the EAE mice, subtle, undetected disruptions between the myelin sheath and axon could be responsible for the loss of AIS protein clustering. To determine whether disrupted axon-myelin interaction could compromise AIS protein clustering, we analyzed AIS length and number following demyelination of the cortex using the curizone model. Exposure of the neurotoxicant, cuprizone (bis-cyclohexanone-oxaldihydrazone), to young adult C57BL/6 mice induces a synchronous and consistent model for demyelination followed by remyelination of the 5th layer of the cerebral cortex (Mason et al., 2001; Matsushima and Morell, 2001; Skripuletz et al., 2008)

6-week-old mice were fed ground chow mixed with cuprizone following a previously described protocol (Hiremath et al., 1998; Dupree et al., 2004). Treated

animals were removed from cuprizone after 3 or 5 weeks for tissue processing and analysis, while an additional group was maintained on cuprizone for 5 weeks followed by an additional 3 weeks on normal (non-cuprizone) chow.

Cuprizone induced demyelination does not disrupt AIS structure:

A qualitative assessment of myelin basic protein (MBP) immunolabeling of cortical layer V, to assess for myelination, revealed reduced MBP levels in mice following 3 weeks of curizone exposure. Following 5 weeks of cuprizone exposure, MBP levels were further reduced, indicating maximum demyelination. MBP labeling of mice following the additional 3 weeks of normal chow after 5 weeks cuprizone exposure revealed an increase in MBP labeling which is consistent with remyelination of cortical layer V.

Immunolabeling for markers directed against ankyrinG allowed us to visualize the axon initial segments in cortical layer V of cuprizone mice. Quantitative analysis of AIS numbers across 3-week-old, 5-week-old cuprizone mice and 5+3 week old cuprizone + normal chow mice revealed no disruption to the organization of AISs following demyelination. Interestingly, nodes of Ranvier cluster a similar set of proteins as the AIS, yet following demyelination, these proteins, including Na+ channels and ankyrinG, are no longer clustered in the node of Ranvier. In contrast, our AIS findings show that following demyelination these proteins maintain their clustering suggesting that these proteins have differential susceptibility to pathologic events depending on their location along the axon.

In summary, our findings demonstrate that the AIS is compromised in EAE, and this structural disruption is independent of demyelination.

Although these findings are highly intriguing by indicating that axonal pathology may be independent of myelin loss in an inflammatory environment, these data are limited to animal models. Here, we will investigate whether similar AIS structural disruption occurs in human MS tissue.

Figure 4. AISs are not disrupted following cuprizone-induced demyelination. Cortical demyelination was assessed by immunolabeling for MBP (A-E). No myelin loss was detected following 1 week of cuprizone treatment (B). Note a slight reduction in MBP labeling following 3 weeks of cuprizone exposure (compare A and C) with a continued decrease in labeling by 5 weeks of treatment (D). Following an additional 3 weeks without cuprizone, MBP labeling increased consistent with remyelination (E). Ankyrin-G labeling of cortical layer V axon initial segments (AIS) revealed no difference among mice that were maintained on ground chow without cuprizone (F) and mice maintained on cuprizone for 1 week (G), 3 weeks (H), 5 weeks (I), or 5 weeks with an additional 3 weeks of recovery (J). Quantitative analysis confirmed that neither AIS number (K) nor AIS length (L) was altered following cortical demyelination at any exposure time point or as compared to untreated (naïve) mice.

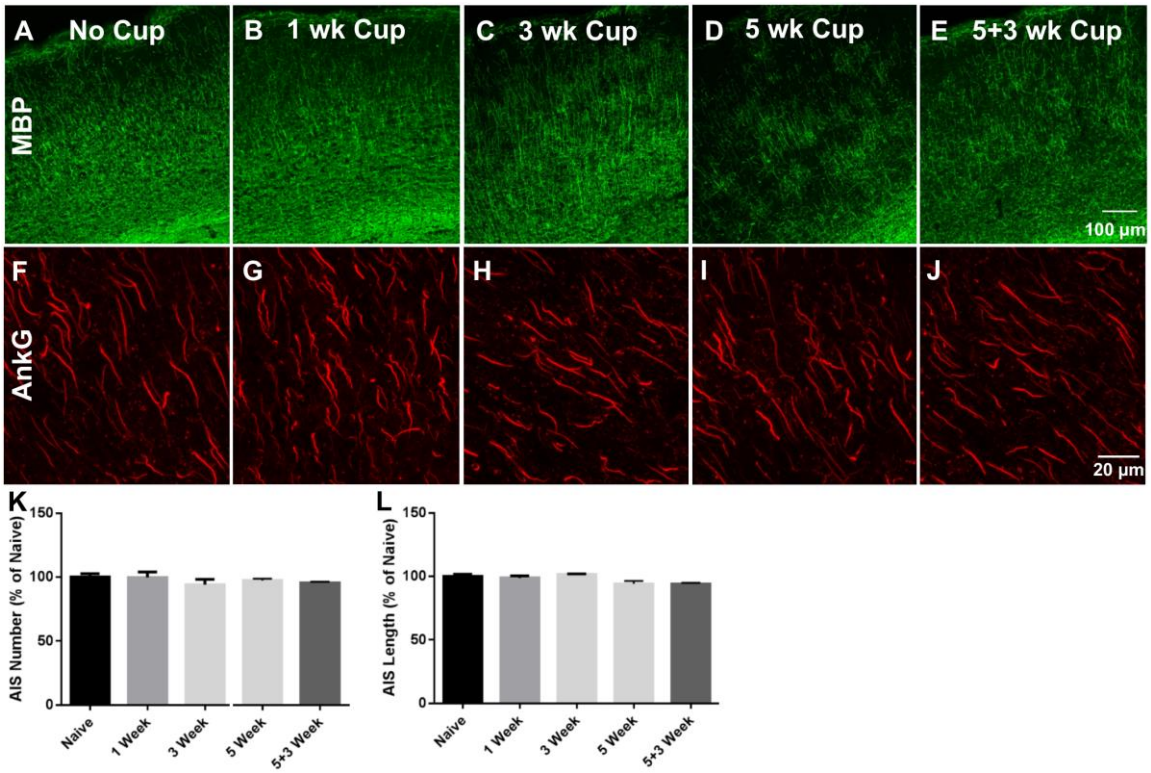
A No Cup
B 1 wk Cup
C 3 wk Cup
D 5 wk Cup
E 5+3 wk Cup
MBP
100 µm
F
G
H
I
J
AnkG
20 µm
K
AIS Number (% of Naive)
150
100
50
0
Naive
1 Week
3 Week
5 Week
5+3 Week
L
AIS Length (% of Naive)
150
100
50
0
Naive
1 Week
3 Week
5 Week
5+3 Week

Figure 4

MATERIALS AND METHODS

Tissue:

Unfixed cortical samples from multiple sclerosis (MS) and non- multiple sclerosis (MS) brains were obtained from the Rocky Mountain Multiple Sclerosis Brain Bank Center. The samples were stored in a freezer at -80°C. The sample information included patient age, sex, sample type, hours between death and tissue harvest, and post-mortem pathological evaluation (Table 1). The samples were inspected at VCU by a neurologist (Unsong Oh, M.D.) and pathologist (Christine Fuller, M.D.) and samples identified to be gray matter were collected. One 20mm x 15mm x 3mm specimen of gray matter from each sample was dissected and stored in a 25mm x 20mm x 5mm Tissue-Tek® Cryomold® (Sakura Finetek USA. Torrance, CA) standard, and frozen in Optimal Cutting Temperature (OCT) compound (Sakura Finetek USA, Torrance, CA), to be used for immunocytochemistry. Another 20mm x 20mm x 5 mm specimen of gray matter from each sample was collected and processed for western blot analysis.

Table 1. Donor information for the Rocky Mountain Multiple Sclerosis Centre brain samples used in this study

Disease Summary	Sample Number	Age	Gender	HTTC	Pathological Evaluation of the Brain
MS	299	51	M	-	Widespread, chronic, inactive plaques
MS	192	81	F	3	-
MS	307	61	F	-	Extensive, remote, chronic, inactive plaques
Control	352	75	F	4.75	Normal cellularity with minimal edema
MS	324	66	F	2.5	Widespread and coalescent demyelinative plaques
MS	344	64	F	5.5	Well demarcated, chronic plaques with cerebral atrophy
Control	486	64	M	13.5	Normal cellularity
Control	102	21	M	65.5	Bilateral hemorrhagic infarcts in pareitooccipital regions
MS	438	75	F	19.5	Massive periventricular plaque burden with corpus callosum atrophy
MS	441	61	F	-	Marked cerebral atrophy with massive plaque burden in periventricular regions
MS	436	-	-	-	-
MS	448	-	-	-	-
Control	101	-	-	-	-
Control	100	-	-	-	-

MS = multiple sclerosis; HTTC = hours to tissue collection; - = data not available (NA)

Immunocytochemistry:

Antibodies:

The mouse monoclonal antibody directed against ankyrinG (ankG) (NeuroMab, Davis, CA; N106/36; dilution of 1:200), and mouse monoclonal antibody directed against neurofascin (Nfasc) (NeuroMab, Davis, CA; L11A/41; dilution of 1:1000) were used to label the axon initial segments. Microglia were labeled with a mouse monoclonal antibody directed against CD 45 (AbD Serotec, Raleigh, NC; dilution of 1:500), a rabbit polyclonal antibody directed against the ionized calcium binding adaptor molecule 1 (IBA-1) (Wako Chemicals USA, Richmond, VA; 1:1000), or a mouse monoclonal antibody human leukocyte antigen DR (HLA DR) (Dako, Ely, UK; dilution of 1:1000). Myelination of cortical tissue was visualized using a mouse monoclonal antibody directed against 2',3'-cyclic-nucleotide 3'-phosphodiesterase (CNP) (Covance, San Diego, CA; SMI 91R, dilution of 1:1000), and mouse monoclonal antibody directed against myelin basic protein (MBP) (Covance, Chantilly, VA; dilution of 1:1000). Mouse monoclonal antibody directed against ankyrinG (ankG) (generous gift from Dr. Manzoor Bhat, University of Texas - San Antonio Health Science Center) was used for western blotting. All secondary antibodies were fluorescently tagged with fluorochromes with excitation wavelengths of 405nm, 488nm or 594nm obtained from Invitrogen Life Technologies (Grand Island, NY; Alexa™ Fluor) and used at a dilution of 1:500.

Number of Samples:

The number of MS and non-MS samples used for ankyrinG and IBA-1 immunocytochemistry is as follows: MS (n=9), non-MS (n=4). The number of samples used for CNP immunocytochemistry is as follows: MS (n=4), non-MS (n=4). The number of samples used for CD45 immunocytochemistry is as follows: MS (n=9), non-MS (n=3). The number of samples used for MBP immunocytochemistry is as follows: MS (n=4), non-MS (n=3). The number of samples used for HLA-DR, Nfasc, and CD 68 immunocytochemistry is as follows: MS (n=2), non-MS (n=2).

Tissue Processing:

Gray matter samples of MS and non-MS tissue were frozen in OCT freezing compound and placed in a Leica CM 1850 UV cryostat for sectioning. The samples were placed on the cutting block, with the desired side facing upwards. 40µm thickness sections (10 sections per sample) were sectioned and mounted on ProbeOn™ Plus microscope slides (Fisher Scientific, Waltham, MA), one section per slide. The slides were labeled and stored in a freezer at -80°C.

Immunofluorescent labeling:

Sections were removed from the -80C freezer, and air-dried for 30 minutes to ensure adhesion to the slide during subsequent steps. Excess OCT was trimmed from the periphery of the slide and a PAP pen (Daido Sangyo, Tokyo, Japan) was used to apply a hydrophobic border around the tissue. For labeling with IBA-1, MBP

and Nfasc primary antibodies, the slides were immersed in 4% paraformaldehyde for 1 hour to fix the tissue. Slides were then immersed in -20°C acetone (Fisher Scientific; Pittsburg, PA) for 10 minutes, washed 3 times in phosphate-buffered saline (PBS) (0.1 M, pH 7.4; 8g of NaCl + 0.2g of KCl + 1.44g of Na2HPO4 + 0.24g of KH2PO4) and blocked in a solution of PBS, 0.5% Triton X-100 (MP Biomedicals; Solon, OH) and 10% cold water fish gelatin (Electron Microscopy Services; Hatfield, PA) for 15 minutes at room temperature. The blocking solution was slightly modified for MBP labeling as 1% Triton X-100 was used instead of the routine 0.5% concentration. Sections were incubated overnight at 4°C in the appropriate primary antibodies diluted in the blocking solution. One the following day, the sections were rinsed 3 times in PBS, blocked for 15 minutes at room temperature and incubated in the appropriate fluorescently labeled secondary antibody, which is dependent on the host species of the primary antibody. Secondary antibodies were diluted 1:500 in the blocking solution and applied to the sections for 90 minutes. Following the secondary antibody incubation, sections were rinsed 3 times in PBS, incubated in BisBenzimide (Sigma-Aldrich, St. Louis, MO, 1:1000 for 2 minutes diluted in PBS) to label nuclei, rinsed 3 times in PBS and mounted with a coverslip (Fisher Scientific, Waltham, MA) using the antifade solution VectaShield™ (Vector Laboratories; Bulingame, CA), and stored at -20°C until imaged. Images not imaged within 1 week of staining were stored in a freezer at -80°C.

Confocal Microscopy Imaging:

Samples were first visualized using a Zeiss AxioImager A1 fluorescence microscope (Carl Zeiss Microscopy, LLC, Thornwood, NY) to ensure that the immunocytochemistry was effective and to confirm correct orientation of the sections. All images for qualitative and quantitative analyses were taken with a Zeiss LSM 710 confocal laser-scanning microscope (Carl Zeiss Microscopy, LLC, Thornwood, NY). Images were collected and compiled as maximum projection z stack images consisting of 50 optical images spanning 25µm of tissue. The collection of 50 images was determined based on Nyquist sampling, 1 Airy disc unit pinhole, using a 40x oil immersion objective with a numerical aperture of 1.3 Images were captured at 1908x1908 pixels using a scan average of 2. Each microscopic field dimension was 215µm x 215µm x 25 µm and each field of view (FOV) collected had a negligible area without tissue present. Gray matter regions were initially confirmed based on cell density and pattern of lipofuscin labeling. Non-overlapping images were taken only from gray matter regions. Between 4-6 images were collected per section. For 405nm excitation, wavelengths between 440-470 were collected. For 488nm excitation, wavelengths between 505-530 nm were collected. For 594nm excitation, wavelengths between 610-650 nm were collected.

Spectral unmixing is a technique used to separate and omit autofluorescent wavelengths originating from lipofuscin pigment from the fluorescent wavelengths of interest originating from the antibody tags (Figure 5). Autofluorescence elimination facilitated quantitative analysis by removing non-specific fluorescence. Spectral unmixing was performed in real time during image capture. All microscopy

Figure 5. Spectral unmixing microscopy. Immunocytochemistry image of axon initial segments labelled with ankG antibody (red lines) and background autofluorescence emanating from lipofuscin pigment (green), shown prior to spectral unmixing (A). Channels are then separated by spectral unmixing to remove unwanted background autofluorescence (C) from the desired image, visualizing the AIS (B).

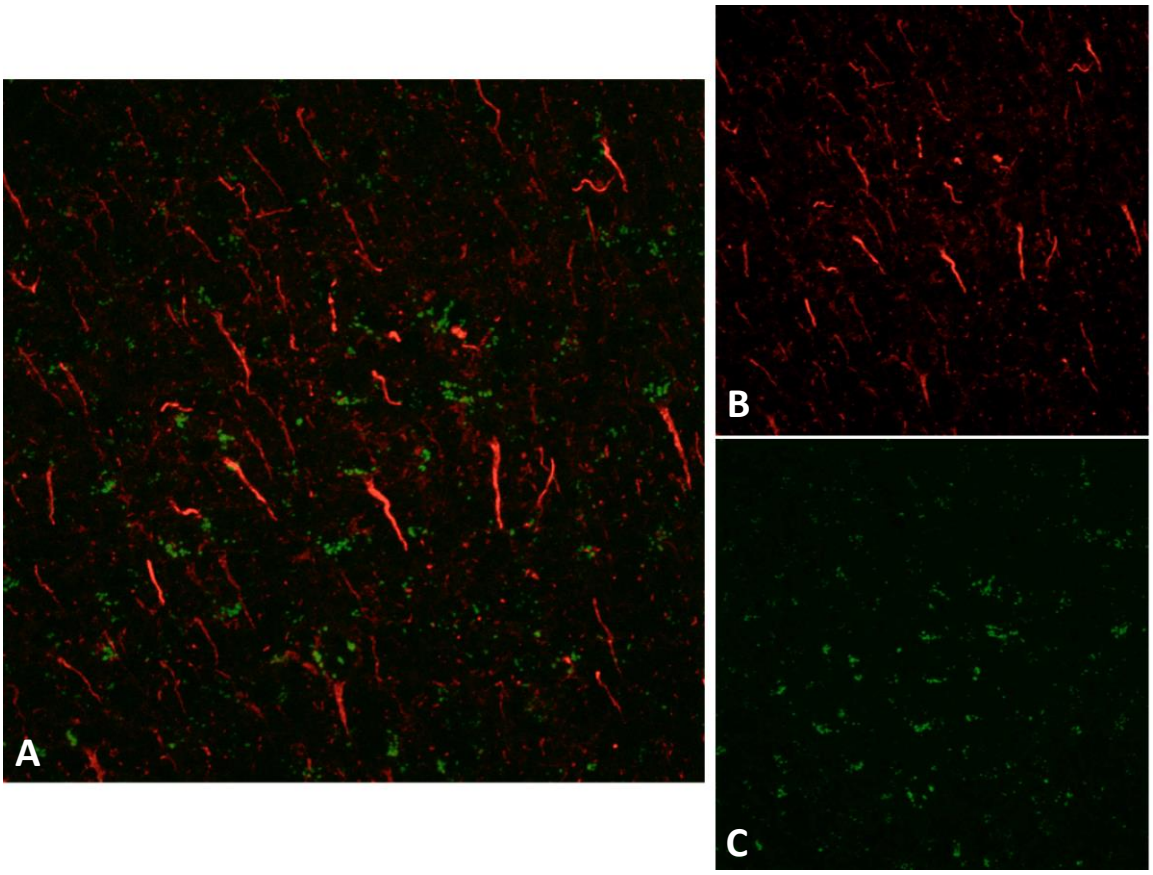

Figure 5

was performed at the Virginia Commonwealth University Department of Anatomy and Neurobiology Microscopy Facility.

Quantitative Image analysis:

The mouse monoclonal antibody directed against the cytoskeletal scaffolding protein ankyrinG was used to visualize the axon initial segments (AIS). AIS quantification was performed by counting the number and measuring the length of the AIS using the ImageJ software (U. S. National Institutes of Health, Bethesda, MD). The maximum intensity projection images were opened in ImageJ and the AISs were manually traced, using the trace tool. Pixels were the units of trace length measured by ImageJ. As each FOV represented 215µm x 215µm of tissue, and measured 1908 pixels x 1908 pixels, 1µm tissue = 8.9 pixels of the image. Red lines of > 5 µm (i.e. > 45 pixels) were considered AISs and were traced. Punctate labeling of < 5 µm (i.e. < 45 pixels) was considered to be nodes of Ranvier and were not traced, as it has been shown that nodes of Ranvier are less than 3 µm long (Dupree et al., 1998). The lengths of the AISs, were logged using the 'measure' key. To eliminate AISs that extended beyond the boundaries of the captured FOV, which would result in an artificial shortening of the segment, initial segments touching any of the six edges of the collected z-stack image were excluded from analysis. Data for both AIS length and number were averaged per sample and a single average for length and for number was used for statistical analysis. To compare the number of AISs, the data are represented as a percent of non-MS (% non-MS ± SEM). The data were

determined to be not normally distributed and thus an unpaired t-test with Welch's correction was performed. To compare AIS length, the average length of the AISs in microns is presented as mean ± SEM. AIS lengths were compared and tabulated in a length distribution graph. Images collected using other antibodies (Nfasc, CD45, MBP, CNP, IBA-1, HLA DR, CD 45, CD 68) were saved as maximum intensity projections and were surveyed and qualitatively assessed using microscopy and ImageJ. All graphing and statistical analyses were performed using GraphPad Prism version 6.03 for Windows (GraphPad Software, San Diego, CA USA).

Western Blot Analysis

Tissue processing:

Samples taken for western blot processing were placed in a 30ml Dounce glass homogenization tube and placed on ice. Lysis buffer (Schafer et al, 2009) (0.32M sucrose + 5mM sodium phosphate monobasic + 10mM EDTA + 0.1% SDS) and 10 µl/ml of the protease inhibitor cocktail (Sigma-Aldrich; P8340; St. Louis, MO)) was added and each sample was homogenized using a Glas-Col® motorized metal handled pestle tissue homogenizer (Glas-Col® Terre Haute, IN) at a motor speed of 60 for ten strokes (1 stroke defined as one full motion of the pestle moving from the top of the Eppendorf tube, to the bottom and back to the top). The homogenate was then centrifuged at 600G and 4°C for 10 minutes in a tabletop Eppendorf Centrifuge 5402 (Eppendorf North America, Hauppauge, NY). The supernatants were collected and stored at -20°C.

Protein assay:

A protein assay was performed to determine the protein concentrations of the homogenized samples facilitating equivalent protein loading onto the gel. Bovine serum albumin (BSA) standards were prepared using serial dilutions of BSA stock with PBS, as per the Micro BCA Kit protocol (Thermo Scientific, Rockford, IL; Thermo#23235). 25 µl of BSA standards and 25 µl of 1:10 diluted MS and non-MS samples were added in triplicates to a 96 well plate. The BCA assay kit reagents A, B and C were then mixed together in a 25:24:1 ratio and 200 µl of the reagent mix was added to each of the occupied wells. The well plate was incubated at 37°C and cooled for 5 minutes before being read in a spectrophotometer. The standard curve was determined and used to calculate protein concentrations.

Western Blot Protocol:

Protein concentrations across samples were normalized by diluting them with sample buffer (Lamelli sample buffer: beta-mercaptoethanol, 20:1) to ensure loading of 20µg of protein per lane. The samples were boiled for 5 minutes, cooled on ice, centrifuged and vortexed prior to loading the gel (Criterion™ TGX™ 18 well precast gel 4-15%). 10µl of molecular weight marker (Bio-Rad, Hercules, CA; Precision Plus Protein™ Kaleidoscope™) was added to the first lane. Western blot apparatus (Biorad Miniprotean Tetracell; Bio-Rad, Hercules, CA) was filled with running buffer (0.1 Tris-Glycine + 1g sodium dodecyl sulfate (SDS) and the gels were run at 70V for 30 minutes to allow the protein to stack, and then at 100V for an additional 1 hour. The gels were then removed and rocked in cold transfer buffer

(10x Tris-Glycine:Methanol:DI H_2O, 1:2:7) for 15 minutes. A nitrocellulose membrane was cut to fit the gel and rocked in cold transfer buffer for 15 minutes. The transfer cassette was made by sandwiching the gel and nitrocellulose membrane between 2 blotting papers and 2 sponges. The gel was then allowed to transfer in a gel box on ice at 100V for 2 hours. Following the transfer, the nitrocellulose membrane was washed in PBS, and incubated in blocking solution (3% non-fat dry milk:PBST, 1.5g:50ml) for 40 minutes. The membrane was incubated overnight in the primary antibody (ankyrinG; 1:2500) diluted in the blocking solution at 4°C. The following day, the membrane was washed in PBS 3 times for 10 minutes each, blocked for 20 minutes, and incubated in a secondary antibody solution for 1.5 hours. The secondary antibody solution consisted of an anti-mouse antibody conjugated with horseradish peroxidase (HRP) (1:5000), and Strep-Tactin HRP conjugate (1:10000). After two 5-minute rinses in phosphate buffered saline tween (PBST) (50ml of PBS+ 250µl of 10% Tween) and four 10-minute PBS rinses, the membrane was incubated in the chemiluminescence reagent (Millipore Corporation, Billerica, MA; Immobilon Western Chemiluminescent HRP Substrate) for 5 minutes. The membrane was then transferred to the film cassette and developed using a Futura 2000 K automatic x-ray film processor (Fisher industries, Dickinson, ND). The western blot films were qualitatively assessed on an x-ray viewer and scanned for documentation.

RESULTS

The axon initial segment (AIS) is the site responsible for action potential initiation and modulation (Meeks et al., 2007; Rasband, 2010). Alterations in the structure of this domain result in the disruption of impulse generation (Schafer et al., 2009). Previous studies from our lab (Clark et al., in review), using the Experimental Autoimmune Encephalomyelitis (EAE) murine model, which replicates many of the inflammatory aspects of Multiple Sclerosis (MS) (DeVries et al., 2012; Secor McVoy et al., 2015; Dupree et al., 2015), demonstrate a reduction in AIS numbers and length (Clark et al. in review). Interestingly, altered AIS numbers and length temporally correlate with poorer clinical scores in EAE mice and imply compromised neuronal function. Although EAE is a model of MS, it is not an exact replica of the disease (DeVries et al., 2012; Secor McVoy et al., 2015; Dupree et al., 2015). Therefore to determine whether AIS numbers and AIS lengths are altered in the human disease, immunocytochemistry was performed on cortical gray matter samples from both groups. To visualize the AISs, cortical samples were immunolabeled with the ankyrinG antibody. AnkyrinG is prominent component of the AIS and is known as the AIS master organizer (He et al., 2013; Kordeli et al., 1995; Jenkins and Bennett, 2001; Sobotzik et al., 2009; Hedstrom et al., 2008; Dzhashiashvili et al., 2007; Zhou et al., 1998). Samples were counterstained with the marker bis benzimide to label the nuclei.

No difference in cell number was observed between MS and non-MS samples:

Since neuronal pathology is a known component of the MS disease process, we attempted to evaluate neuronal cell loss in MS and non-MS samples. For this approach, we employed the neuron specific marker NeuN (Saaltink et al., 2012; Gómez-Nicola et al., 2013; Smolders et al., 2013). Unfortunately, NeuN did not label the human tissue. As an alternative approach, we used bis benzimide as an indicator of cell number. Bis benzimide is not specific to neurons and labels the nucleus of all cell types. Using this nuclear marker, we quantitatively compared total cell number between MS and non-MS samples. As shown in Figure 6, no difference in the number of bis benzimide labeled cells was observed between MS and non-MS groups. Although not specific to neurons, these counts indicate that cell loss is not observed in the MS samples.

The number of axon initial segments are not significantly reduced in MS:

To evaluate AIS number in MS and non-MS samples, the number of ankG positive profiles, greater than 5um, was determined per field of view. As seen in Figure 7, images from MS and non-MS samples reveal AISs labeling with the ankG antibody. AIS counts revealed a 40% reduction in the number of AISs between the MS and non-MS samples. Although quantitation indicated a 40% reduction in AIS number, statistical analysis indicated that this reduction was not significantly different (Figure 8). A less stringent statistical analysis, considering each field of view to be an independent 'n' number, revealed a statistically significant reduction of AISs in MS by 40% (p=.001134) compared to non-MS (Figure 9)

Figure 6. No difference in cell numbers between MS and non-MS. The number of nuclei, as stained by bis benzimide, of MS samples as a percentage of non-MS revealed no difference in the number of cells within MS and non-MS cortex samples.

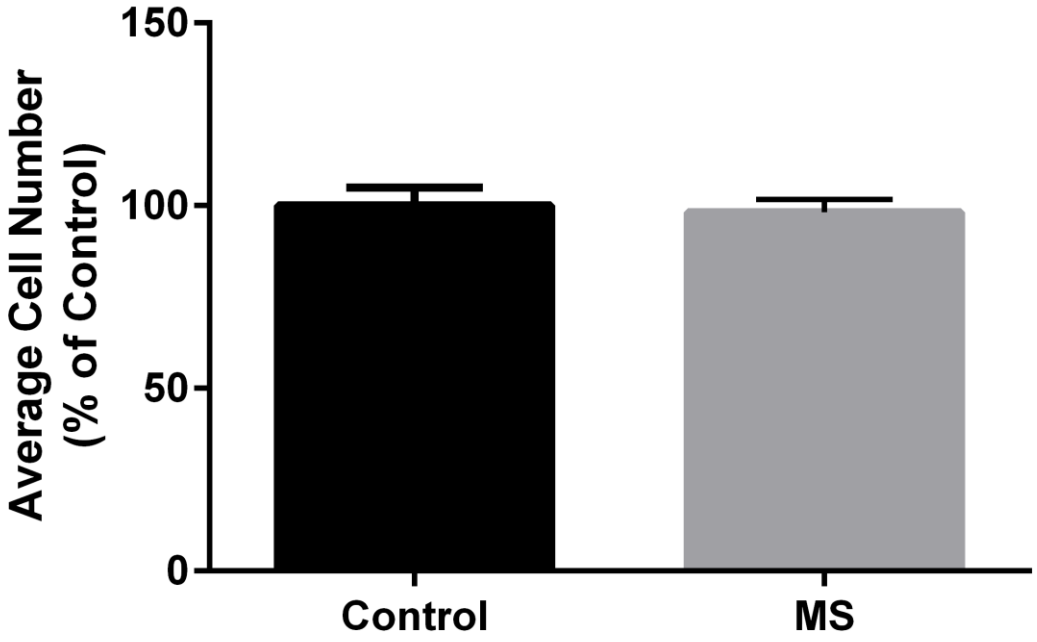

Figure 6

Figure 7. Sample immunocytochemistry images representative of AIS data. Immunocytochemistry of Non-MS tissue (panel A) and MS tissue (panel B). AnkyrinG labelled Axon initial segments (AIS) are shown as red lines (white arrows). The bis benzimide labelled nuclear regions are shown in blue. The red blotches are background noise caused by lipofuscin autofluorescence.

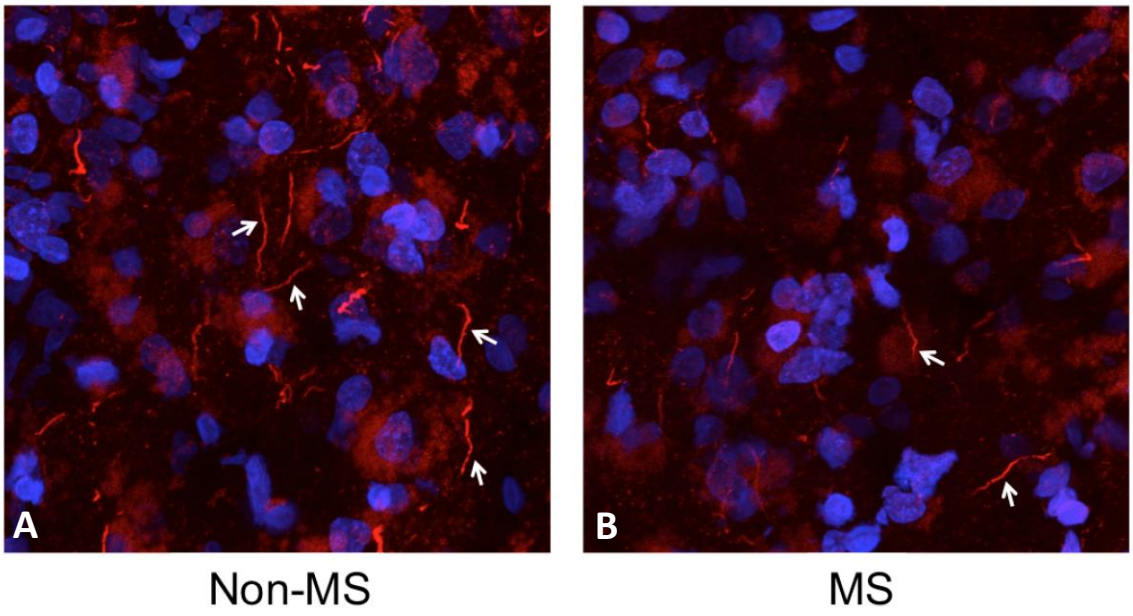

Figure 7

Figure 8. Axon initial segment numbers in multiple sclerosis compared to non – multiple sclerosis cortical tissue

AIS numbers of MS samples as a percentage of non-MS shows a ~40% reduction (P value = 0.1934)

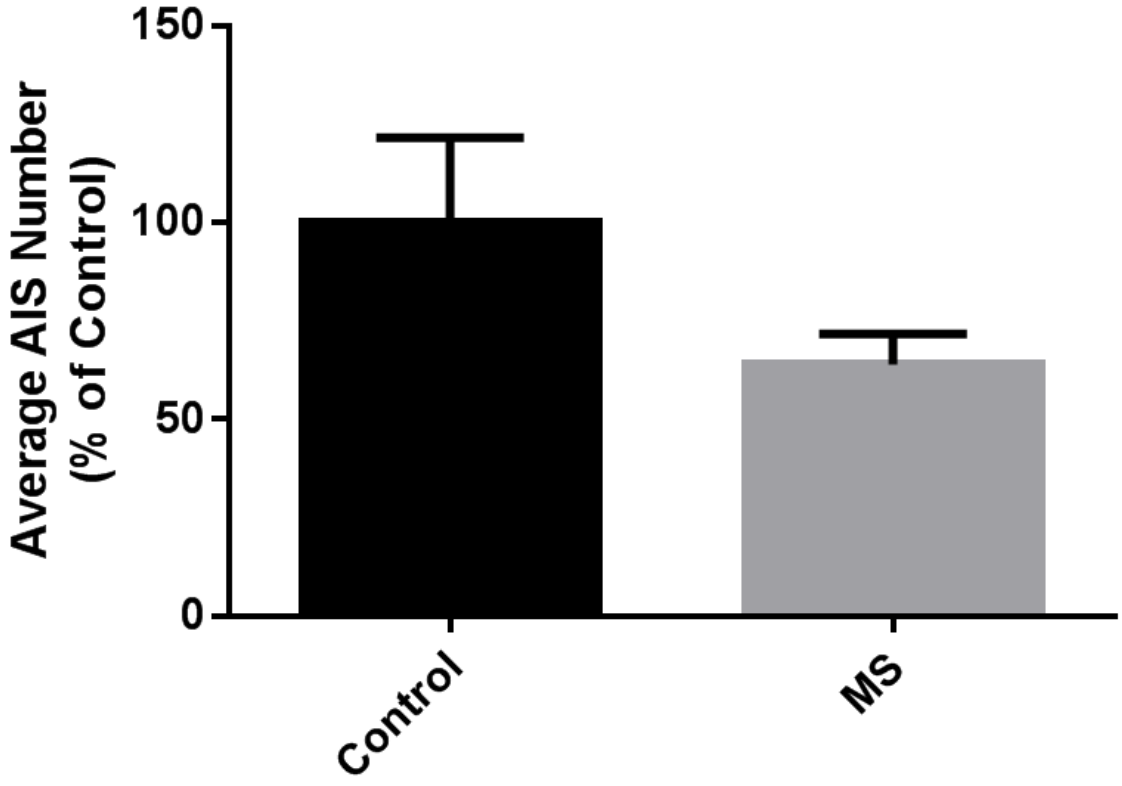

Figure 8

Figure 9. Axon initial segments in multiple sclerosis compared to non-multiple sclerosis using each field of view as an individual n number.

AIS numbers of MS samples as a percentage of non-MS shows a ~40% reduction (P value = 0.001134)

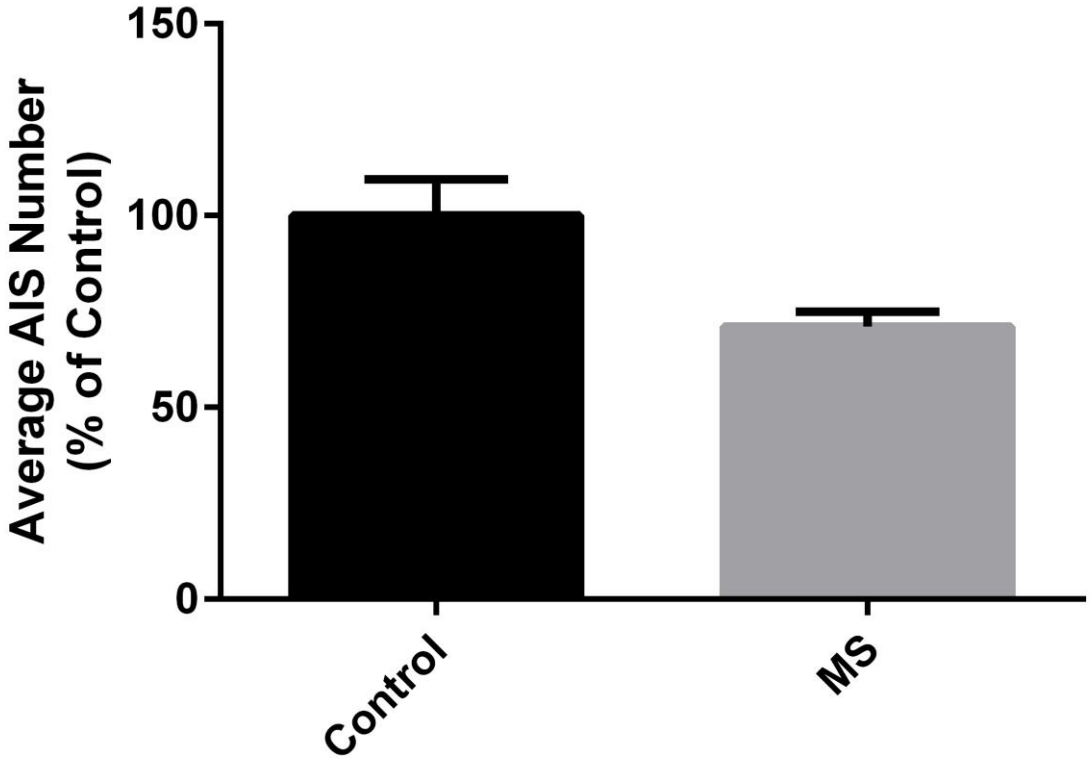

Figure 9

Axon initial segment lengths not reduced in multiple sclerosis:

As presented above, the apparent reduction in the number of AISs in MS samples was not statistically significant; however, changes in AIS length have also been reported to alter AIS function (Adachi et al., 2014; Grubb and Burrone; Kaphzan et al., 2011; Kuba et al., 2010,2012). For example, action potential generation threshold changes with change in length and position of the AIS along the axon. In addition, our lab has previously reported that AIS length is significantly reduced in EAE mice and this reduced length preceded AIS loss. Therefore, I proposed that altered AIS length represents an early pathology of AIS disruption and may present in MS tissue even in the absence of AIS loss. Therefore, I quantitatively compared AIS length between MS and non-MS samples. To investigate potential differences in AIS length between MS and non-MS tissue, we measured the lengths of the ankG labeled AISs in both groups. Consistent with our EAE work, we analyzed AIS average length and compared AISs based on groupings. Regardless comparison approach, statistical analysis revealed no difference in AIS length between MS and non-MS tissue (Figure 10). As expected, the average AIS length was between 10 and 20 um.

Western Blotting to isolate Axon Initial Segment Protein AnkyrinG:

Our AIS number findings were not significantly different according to statistical comparison. Although not significantly different, we observed a 40% reduction. Therefore, we proposed that highly variability among regions may dilute AIS pathology. Therefore, proposed to further investigate AIS protein integrity by

western blot analysis. Western blot analysis provides 2 advantages: 1. Since western blots required homogenized samples, this approach allows a higher throughput method for analyzing multiple brain samples per donor, and 2. Provides higher resolution of pathology, as degradative products of AIS proteins would be easy to visualize even with modest AIS pathology.

Since ankG and its breakdown products have previously been identified by western blotting and quantified by densitometric analysis (Kordeli et al., 1995; Schafer et al., 2009; Phillips et al., 2010), we focused out efforts of this protein for our western blot analysis. As shown in Figure 11, the western blot showed protein bands at the molecular weights expected to see ankyrinG, at ~480 and ~200 kDA.. Interestingly, these bands were observed in two non-MS samples (n=3), but were present in only one MS sample (n=4). Bands were found at ~75 kDA as well, where we would expect to find ankyrinG breakdown products (Schafer et al., 2009; Phillips et al., 2010).

No correlation between Axon Initial Segment loss in Multiple Sclerosis and tissue myelination:

Myelin has been shown to play an integral role in the maintenance of the structure of the Node of Ranvier (Eshed-Eisenbach and Peles, 2013; Susuki et al., 2013; Dupree et al., 1999). The node of Ranvier and the AIS have a highly similar ion channel composition and organization (Rasband, 2010; Kole et al., 2008). While this

Figure 10. Axon Initial Segment lengths comparable between MS and non-MS cortical tissue

Length distribution graph comparing AIS lengths of MS and non-MS tissue. While the highest number of AIS lengths ranged between 10 – 20 µm, and the lowest number of AIS lengths were over 30 µm, a comparison across all AIS length subgroups, revealed no noticeable difference in AIS length between MS and non-MS tissue.

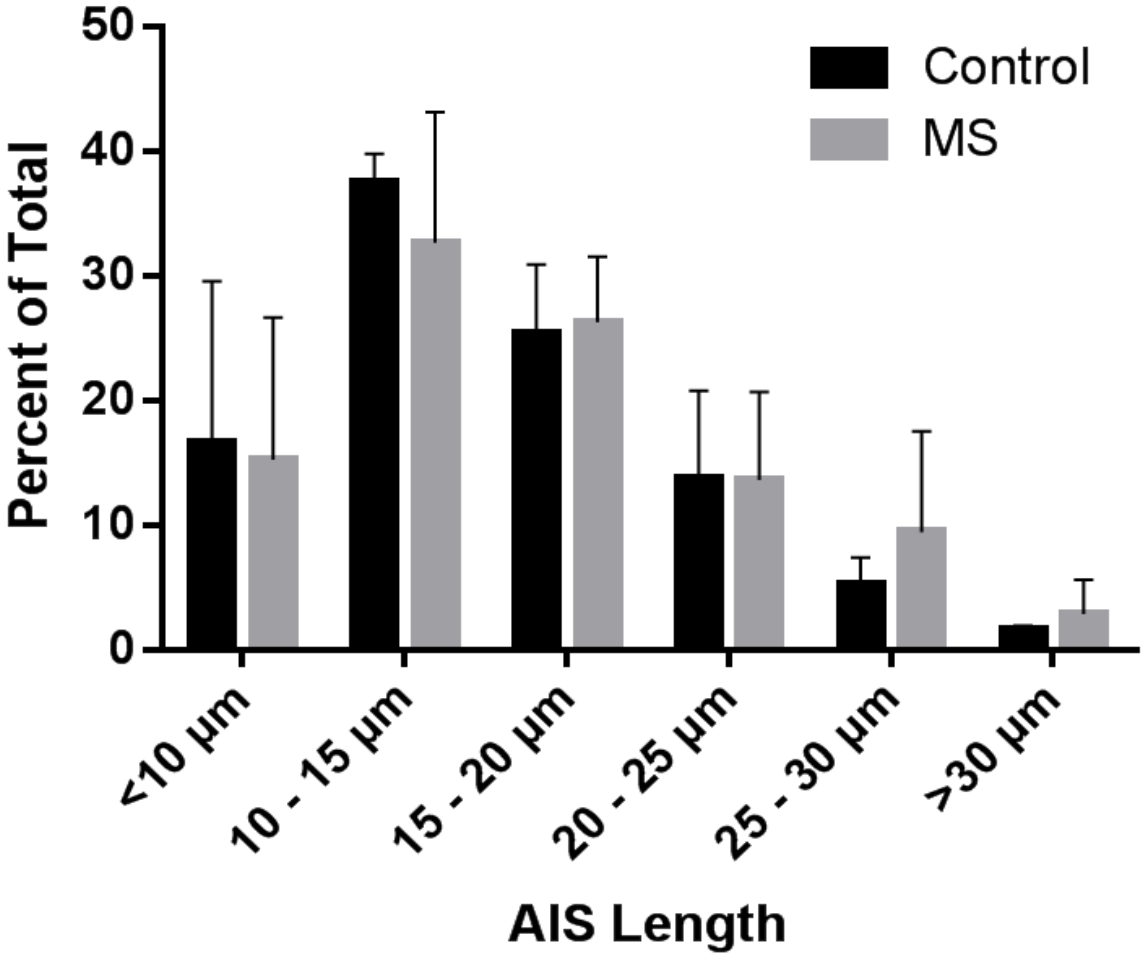
50
40
30
20
10
0
Percent of Total
Control
MS
<10 µm
10 - 15 µm
15 - 20 µm
20 - 25 µm
25 - 30 µm
>30 µm
AIS Length

Figure 10

Figure 11. Western Blot analysis of Ankyrin G in MS and non-MS tissue. Western blot film labeled with Ankyrin G antibody revealed bands at ~480 kDa and ~200 kDa molecular weights, where full length isoforms of Ankyrin G are expected to be seen. Non-MS samples (n=3) revealed two bands while MS samples revealed only one (n=4). Bands seen at ~75 kDa correspond to potential Ankyrin G breakdown products

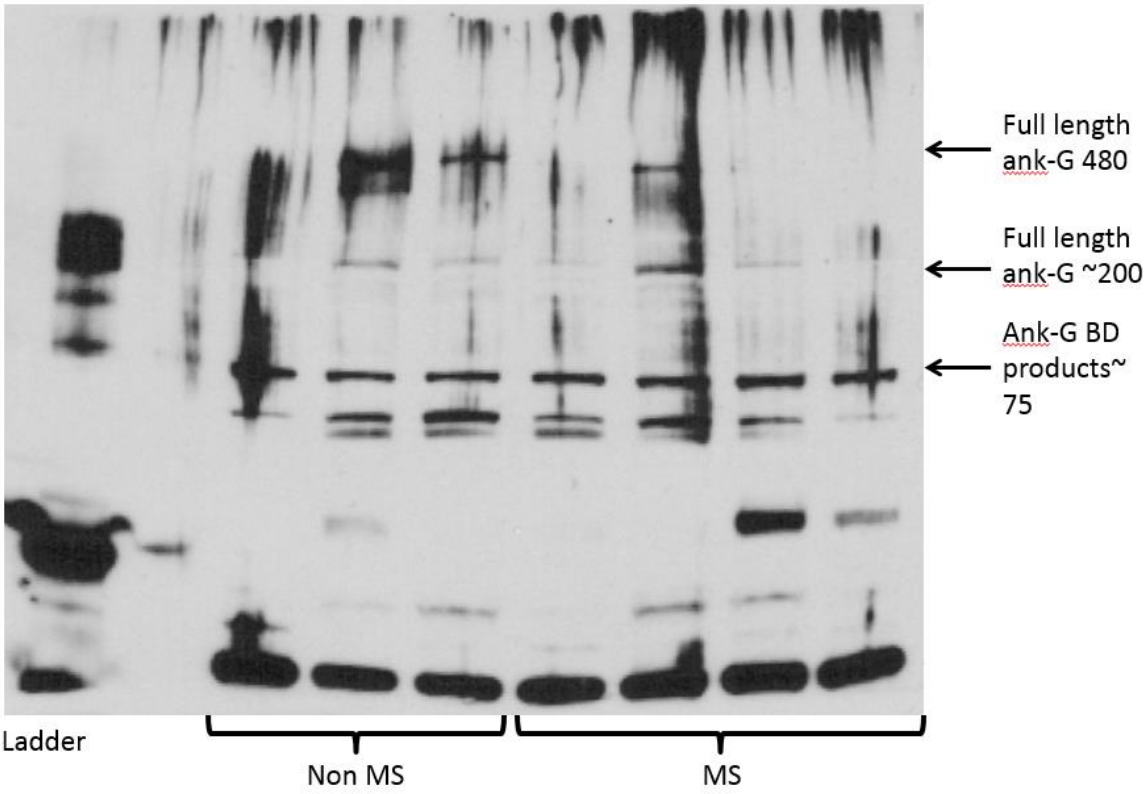
Full length ank-G 480
Full length ank-G ~200
Ank-G BD products~ 75
Ladder
Non MS
MS

Figure 11

would indicate a similar vulnerability of the AIS to the state of myelination of the neuron, previous studies in our lab (Clark et al., in review) and others (Hamad and Kole, 2015), using the Cuprizone mouse model of demyelination (Mason et al., 2001; Matsushima and Morell, 2001; Skripuletz et al., 2008), have demonstrated that the AIS structure is maintained in demyelinated states. Although studies indicate that AIS stability is not dependent on myelination in rodents, we determined whether the state of myelination regulates AIS stability or AIS protein stability in human tissue. For this study, we employed immunocytochemistry using the cyclic nucleotide phosphodiesterase (CNP) antibody to label myelin in MS and non-MS tissue. After selecting 4 MS and 4 non-MS samples that were representative of the trend seen in our previous AIS quantification analysis, we triple labeled non-MS and MS tissue samples with CNP (myelin marker), ankyrinG (AIS marker) and bisbenzimide (nuclear marker), as seen in Figure 12. Qualitative analysis of the images confirmed our previous findings of an apparent decrease in AIS number in MS tissue compared to non-MS tissue. Interestingly, although the MS samples consistently presented fewer AISs, this reduction was independent of the extent of myelination. As observed in Figure 12, qualitative analysis revealed that the number of AISs was reduced in demyelinated plaques (Figure 12-C) or in normal appearing grey matter (Figure 12-B). These findings suggest that the apparent reduction in AIS number observed in MS does not correlate with the state of cortical myelination.

Figure 12. No change in AIS numbers between myelinated and demyelinated MS tissue. Immunocytochemistry of non-MS (A) and MS (B & C) tissue labelled with CNP antibody (green), a myelin marker, Ankyrin G antibody (red), an AIS marker, and bis benzimide (blue), a cellular nuclei marker. Non-MS tissue (A) showed a noticeably higher number of AIS compared to all MS tissue. Myelinated MS tissue (B) when qualitatively compared with demyelinated MS tissue (C), showed no observable difference in AIS number, indicating that the lowered AIS counts were not related to the state of myelination of the tissue. Bis benzimide staining once again confirmed a consistent number of cells across all tissue samples.

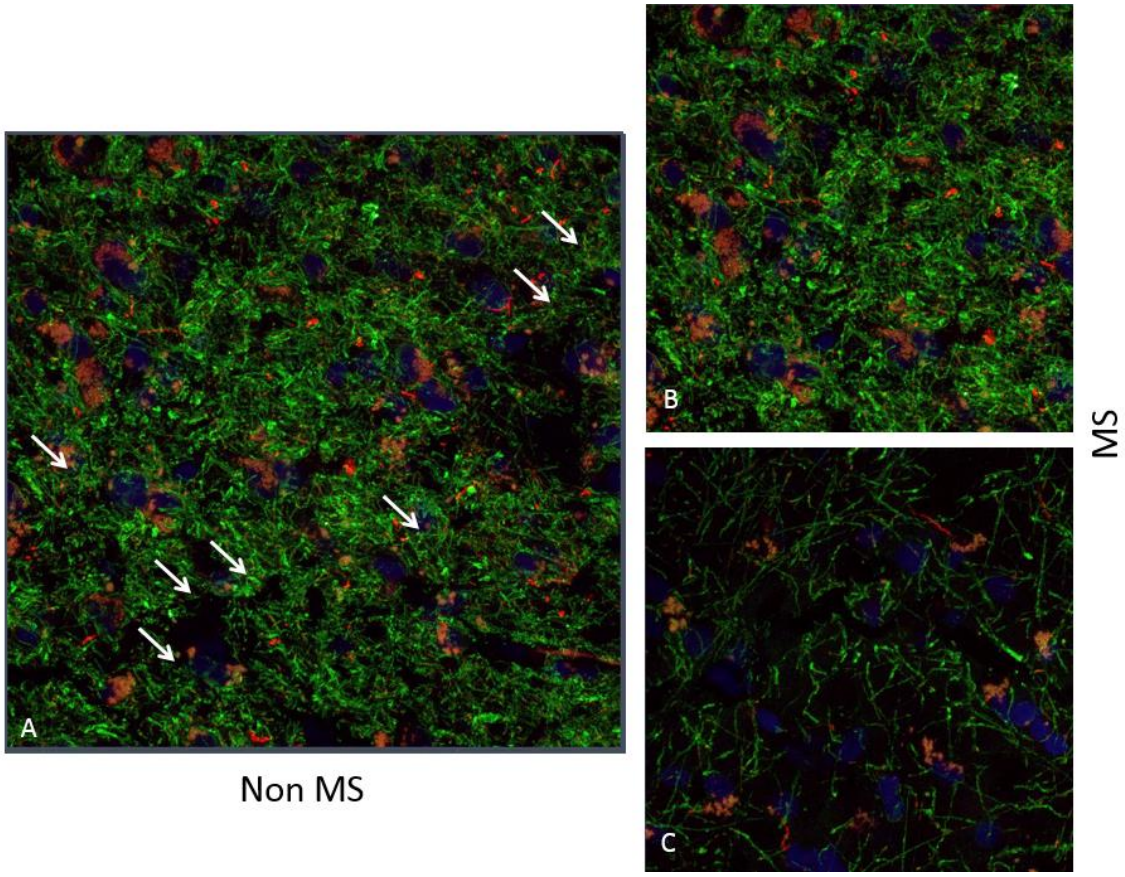

Figure 12

DISCUSSION

The goal of this study was to investigate axon initial segment (AIS) pathology in multiple sclerosis (MS). Data gathered from immunocytochemistry and, to a lesser extent, western blotting has demonstrated that the proteins clustering in the axon initial segment may be compromised in multiple sclerosis. Although the number of AISs was reduced by ~40% in the MS tissue as compared to non-MS tissue, this apparent reduction was not significantly different based on statistical analysis. Consistent with the apparent reduction in AIS number, the western blot findings also suggest a loss of AIS proteins. Quantitation of AIS lengths remained unchanged. Contrary to what we know about the node of Ranvier's susceptibility to demyelination (Dupree et al., 1999; Dupree et al., 2004; Marcus et al., 2006; Pomicter et al., 2010, Dugandžija-Novaković et al. 1995; Salzer et al., 1997; Rasband et al., 1998; Rasband et al., 1999; Tait et al., 2000; Bhat et al., 2001), no correlation between the reduction of AISs and the state of myelination of cortical MS tissue was observed.

Axon initial segment integrity and Multiple Sclerosis :

Axonal pathology is a hallmark feature of multiple sclerosis, as first described by Charcot (reviewed by Kornek and Lassmann, 1999). Axonal damage has been shown to be intimately responsible for many of the characteristic signs and

symptoms of MS, and is proposed as the cause of the progressive neurological decline observed in the later stages of the disease (Trapp and Dutta, 2011; Trapp and Nave, 2008; Haines et al., 2011). Axonal damage, specifically axonal transection, is abundantly observed in both active and chronic cortical lesions in MS, bearing a correlation to both inflammation and demyelination (Ferguson et al., 1997; Trapp et al., 1998). The integrity of axonal domains such as the node of Ranvier (NoR) and the axon initial segment (AIS) are imperative to maintaining proper axonal structure and function (Bhat et al, 2001; Buttermore et al., 2013; Chang and Rasband., 2013). It has been shown by our lab, our collaborators and others that the NoR is compromised in multiple sclerosis and its models (Bhat et al., 2001; Howell et al., 2006; Ishibashi et al., 2002; Pillai et al., 2009; Rasband et al., 1999; Rosenbluth et al., 2003, 2014; Suzuki et al., 2004; Thaxton et al., 2011; Dupree et al., 2004). The NoR and the AIS also have a highly similar protein, and specifically ion channel compositions (Buffington and Rasband, 2011), implying a potentially similar susceptibility of AIS integrity under similar circumstances. Hence, we were interested in investigating the stability of the AIS in multiple sclerosis.

AIS numbers:

Immunocytochemistry of MS and non-MS tissue, labeled AISs and showed a dramatic decrease of AISs (>40%) in MS tissue, compared to non-MS tissue. While these findings are not statistically significant, we think they are of considerable value, as they follow the trend seen in our background studies using murine models of MS. There are a variety of reasons why statistical significance was difficult to

achieve with this study. It is well known that the use of post mortem human tissue in biomedical research is challenging due to several methodological problems. The genetic variability and epigenetic modification of the human genome, make human tissue much more inconsistent than animal tissue in research (Bennett, 2010). This is accentuated by other variables such as age, sex, comorbidities, cause of death, and time till harvest etc., all of which could not be controlled for in this study.

Furthermore, the tissue we had access to for this study was poorly characterized topographically. Information regarding specific cortical layer, cortical location and orientation was not available. Additionally, we have determined, via a post-hoc power of analysis calculation, that the study is underpowered substantially limiting our ability to observe a significant difference between groups. The power of analysis calculation revealed that using samples of similar variability, we would need a total of 68 samples in both MS and non-MS groups to achieve statistical significance in this study. Unfortunately, additional human samples were not available at the time of the study. Recently, we have obtained additional samples from the Netherlands Brain Bank. These samples are well characterized with regard to age at death, gender, age at disease diagnosis, type of disease, clinical history, post mortem harvest time and brain cortical region. Preliminary observations from this new cohort of samples using similar experimental techniques reveals a similar trend as presented in this study

To strengthen our immunocytochemistry results, we conducted western blot analyses of human MS and non-MS tissue employing antibodies directed against ankyrinG. Kordeli et al. (1995) originally found two isoforms of full-length ankyrinG

in the AIS of human cortical tissue, at 480 and 270 kDA. A study performed by Schafer et al. (2009) demonstrated that the calcium-dependent cysteine protease, calpain, mediated AIS breakdown in a stroke model. These authors reported full-length isoforms of ankyrinG and their breakdown products at ~95 and 72 kDa. Phillips et al. (2010) while investigating proteolysis in a diffuse brain injury model, showed full length ankyrinG bands at 212 and 220 kDA with a breakdown product at 75 kDA. Together these studies provide the feasibility of the western blot approach to quantify ankyrinG degradation. Our initial experiments to isolate ankyrinG were inconclusive due to the use of an ankyrinG antibody that was later found to be ineffective at labeling the protein on western blots. While a working ankyrinG antibody was eventually acquired, the quantity was insufficient to effectively optimize the western blot experimental conditions to provide quantifiable results. However, preliminary findings using the human tissue revealed protein bands at the molecular weights expected for ankyrinG: 2 bands with apparent molecular weights of ~480 and ~200 kDA. Furthermore, these bands were seen in two out of three non-MS samples while only one of four MS samples revealed full length banding patterns suggesting that loss of ankyrinG in the MS samples compared to the non-MS samples. Bands were found at ~75 kDA as well, where we would expect to find ankyrinG breakdown products. While highly preliminary, these data augment the immunocytochemistry results indicating a breakdown of ankyrinG in the MS samples.

An important caveat to these findings, however, is that ankyrinG is not limited to AIS clustering. AnkyrinG also clusters in the node of Ranvier. Therefore, it

cannot be definitively concluded that ankyrinG breakdown products observed on the western blots results from AIS breakdown.

AIS lengths:

The AIS is the site of action potential generation and modulation. The AIS is a highly plastic domain, allowing it to regulate nerve excitability via alterations in its length and ion channel density (Yoshimura and Rasband, 2014; Kole and Stuart., 2012; Bender and Trussell, 2012; Kuba., 2012; Ogawa and Rasband., 2008). Previous studies done by our lab using a mouse model of MS, known as Experimental Autoimmune Encephalomyelitis (EAE), have demonstrated changes in AIS length in both acute and chronic disease time points (Clark et at., [in review]). In the EAE experiments, AIS lengths measured from mice, taken at the early time point (3 days post peak clinical symptoms) showed significant shortening of AISs in the EAE tissue, compared to the naive controls, despite no significant reduction in AIS numbers. However, AIS lengths measured from mice, taken at the late time point (9 days post peak clinical symptoms) showed a much less dramatic shortening of AISs, despite showing a significant reduction in AIS numbers. One possible explanation for these findings is that the active inflammatory disease process targets the AIS structure and shortens it over time, leading to its eventual complete disruption. In acute inflammation, AIS are undergoing active degradation and shortening, but are still not lost. As the disease progresses, these AIS are completely lost. We postulate that there is a subfraction of AISs that are resistant to this inflammatory process, accounting for the remaining AISs see in the counts. It would follow that the lengths

of the remaining AISs would be unaltered, by nature of their resistance to inflammatory disruption.

We were interested in investigating changes in AIS dimensions in human MS tissue, and performed a quantitative analysis of AIS lengths in MS and non-MS tissue. Statistical analysis of our data showed no change in AIS length between the two groups. As we did not see a statistically significant reduction in the number of AISs between MS and non-MS tissue, we would not expect to see a significant change in AIS lengths between the two groups. Another possible explanation for the lack of alteration to AIS lengths despite seeing a dramatic reduction of AIS numbers in MS samples is that the remaining AISs found in the MS tissue are resistant to disruption by pathological processes. This is especially accurate since post mortem human samples bear a higher resemblance to late stage EAE than to early stage EAE, when comparing pathogenesis timelines. While the mechanisms surrounding AIS disruption and shortening in these scenarios are not fully understood, we believe that our findings with the human tissue and murine EAE studies warrant further investigation in this area.

AIS integrity is not related to demyelination:

The myelin sheath, produced by the oligodendrocytes in the CNS, envelops the axon and plays a vital role in neuronal functioning. Disruption of the myelin sheath results in disruption of axonal integrity. It has been shown by our lab (Dupree et al., 1999; Dupree et al., 2004; Marcus et al., 2006; Pomicter et al., 2010), and others (Kuba and Susuki., 2015; Rasband and Chang., 2013; Rasband et al., 1999; Tait et al.,

2000; Bhat et al., 2001), that the establishment and maintenance of the node of Ranvier is highly dependent on the presence of myelin. However, despite the compositional and structural similarities between the NoR and the AIS, studies show that the establishment of the AIS is not dependent on myelin (Kuba and Susuki., 2015; Rasband and Chang., 2013; Buttermore et al., 2013). Previous studies done in our lab using the Cuprizone model (a demyelinating/remyelinating murine model) have shown no change in AIS integrity in demyelinated mouse cortical tissue (Clark et al., [in review]). Furthermore, studies performed by our lab using the EAE model (a murine model exhibiting cortical inflammation absent any cortical demyelination), showed that AISs are lost in myelinated cortical tissue. These findings imply that the AIS structure is not dependent on myelin (Clark et al., [in review]).

To determine if this trend is observed in human multiple sclerosis, we attempted to investigate the relationship between AISs and myelin in human MS tissue. Initial attempts to immunolabel the tissue using the antibodies directed against Myelin Basic Protein (MBP) and Myelin Oligodendrocyte Glycoprotein (MOG) were unsuccessful, showing little to no specific staining, as the human tissue in our possession was unfixed, and the antibodies required fixed tissue to effectively label myelin. Post-fixing the tissue yielded no discernable change in the effectiveness of the immunolabelling. Experiments using the antibody 2',3'-cyclic-nucleotide 3'-phosphodiesterase (CNP) resulted in successful labeling of myelin in the unfixed human tissue. Qualitative analysis of the MS and non-MS human tissue showed similar regions of myelination and demyelination across all samples.

Consistent with the idea that AIS disruption is independent of myelin loss, Figure 12 reveals comparable myelin labeling in the MS and non-MS samples while the number of AISs is substantially reduced in the MS samples compared to the non-MS samples. This suggests that AIS loss occurred in the absence of demyelination. Multiple sclerosis, has for decades, been considered a primarily a demyelinating and inflammatory disease, with subsequent axonal pathology. These findings, correlate with our background studies, and are extremely exciting as they suggest that axonal pathology is a primary event in MS, showing a disruption in axonal protein domain organization, independent of demyelination.

In conclusion, while we did not show a statistically significant reduction of axon initial segments in multiple sclerosis, our results highlight a trend, which demonstrates the AISs may be disrupted in MS. We show that axonal pathology is a primary event in MS, as AIS integrity is not related to demyelination. These findings, while preliminary, are highly exciting as they enhance our understanding of what was once considered a prototype demyelinating disease.

REFERENCES

- Acar G, Idiman F, Idiman E, Kirkali G, Cakmakci H, Ozakbas S. Nitric oxide as an activity marker in multiple sclerosis. J Neurol. 2003;250:588-592.
- Aggarwal S, Yurlova L, Simons M. Central nervous system myelin: structure, synthesis and assembly. Trends Cell Biol. 2011;21:585-593.
- Ahlgren C, Oden A, Lycke J. High nationwide prevalence of multiple sclerosis in Sweden. Mult Scler. 2011;17:901-908.
- Akiyama H, McGeer PL. Brain microglia constitutively express beta-2 integrins. J Neuroimmunol. 1990;30:81-93.
- Alizadeh A, Dyck SM, Karimi-Abdolrezaee S. Myelin damage and repair in pathologic CNS: challenges and prospects. Front Mol Neurosci. 2015;8:35.
- Arancibia-Carcamo IL, Attwell D. 2014. The node of Ranvier in CNS pathology. Acta Neuropathol 128:161-175.
- Arroyo EJ, Xu YT, Zhou L, Messing A, Peles E, Chiu SY, Scherer SS. 1999. Myelinating Schwann cells determine the internodal localization of Kv1.1, Kv1.2, Kvbeta2, and Caspr. J Neurocytol 28:333-347.
- Baalman K, Marin MA, Ho TS, et al. Axon Initial Segment–Associated Microglia. The Journal of Neuroscience. 2015;35:2283-2292.
- Baldwin AC, Kielian T. Persistent immune activation associated with a mouse model of Staphylococcus aureus-induced experimental brain abscess. J

Neuroimmunol. 2004;151:24-32.

- Banwell B, Krupp L, Kennedy J, et al. Clinical features and viral serologies in children with multiple sclerosis: a multinational observational study. Lancet Neurol. 2007;6:773-781.
- Bender KJ, Trussell LO. The physiology of the axon initial segment. Annu Rev Neurosci. 2012;35:249-265.
- Bennett V, Lambert S. 1999. Physiological roles of axonal ankyrins in survival of premyelinated axons and localization of voltage-gated sodium channels. J Neurocytol 28:303-318.
- Berghs S, Aggujaro D, Dirkx R,Jr, Maksimova E, Stabach P, Hermel JM, Zhang JP, Philbrick W, Slepnev V, Ort T, Solimena M. 2000. betaIV spectrin, a new spectrin localized at axon initial segments and nodes of ranvier in the central and peripheral nervous system. J Cell Biol 151:985-1002.
- Bhatt A, Fan LW, Pang Y. Strategies for myelin regeneration: lessons learned from development. Neural Regen Res. 2014;9:1347-1350.
- Bitsch A, Kuhlmann T, Da Costa C, Bunkowski S, Polak T, Bruck W. Tumour necrosis factor alpha mRNA expression in early multiple sclerosis lesions: Correlation with demyelinating activity and oligodendrocyte pathology. Glia. New York, N.Y. :2000;29:366-375.
- Bitsch A, Schuchardt J, Bunkowski S, Kuhlmann T, Brück W. Acute axonal injury in multiple sclerosis. Brain. 2000;123:1174-1183.
- Boiko A, Vorobeychik G, Paty D, Devonshire V, Sadovnick D, University of British Columbia MS Clinic Neurologists. Early onset multiple sclerosis: a

longitudinal study. Neurology. 2002;59:1006-1010.

- Boppana S, Huang H, Ito K, Dhib-Jalbut S. Immunologic Aspects of Multiple Sclerosis. Mount Sinai Journal of Medicine: A Journal of Translational and Personalized Medicine. 2011;78:207-220.
- Bosio A, Binczek E, Haupt WF, Stoffel W. Composition and biophysical properties of myelin lipid define the neurological defects in galactocerebroside- and sulfatide-deficient mice. J Neurochem. 1998;70:308-315.
- Bruck W. The pathology of multiple sclerosis is the result of focal inflammatory demyelination with axonal damage. J Neurol. 2005;252 Suppl 5:v3-9.
- Bsibsi M, Ravid R, Gveric D, van Noort JM. Broad expression of Toll-like receptors in the human central nervous system. J Neuropathol Exp Neurol. 2002;61:1013-1021.
- Butovsky O, Jedrychowski MP, Moore CS, et al. Identification of a unique TGF-beta-dependent molecular and functional signature in microglia. Nat Neurosci. 2014;17:131-143.
- Buttermore ED, Thaxton CL, Bhat MA. 2013. Organization and maintenance of molecular domains in myelinated axons. J Neurosci Res 91:603-622.
- Cader S, Cifelli A, Abu-Omar Y, Palace J, Matthews PM. Reduced brain functional reserve and altered functional connectivity in patients with multiple sclerosis. Brain. 2006;129:527-537.
- Calabrese ,Massimiliano, Magliozzi ,Roberta, Ciccarelli ,Olga, Geurts JJ,G.,

Reynolds ,Richard, Martin ,Roland. Exploring the origins of grey matter damage in multiple sclerosis. .

- Carpenter AF, Carpenter PW, Markesbery WR. Morphometric analysis of microglia in Alzheimer's disease. J Neuropathol Exp Neurol. 1993;52:601-608.
- Castellano Lopez B, Gonzalez de Mingo B. Scientific contributions of Pio del Hortega to neurosciences. Neurologia. 1995;10:265-276.
- Chamberlain KA, Nanescu SE, Psachoulia K, Huang JK. Oligodendrocyte regeneration: its significance in myelin replacement and neuroprotection in multiple sclerosis. Neuropharmacology.
- Chang K, Rasband MN. Chapter Five - Excitable Domains of Myelinated Nerves: Axon Initial Segments and Nodes of Ranvier. Current Topics in Membranes. 2013;72:159-192.
- Clark BD, Goldberg EM, Rudy B. Electrogenic tuning of the axon initial segment. Neuroscientist. 2009;15:651-668.
- Coetzee T, Fujita N, Dupree J, et al. Myelination in the absence of galactocerebroside and sulfatide: normal structure with abnormal function and regional instability. Cell. 1996;86:209-219.
- Coetzee T, Suzuki K, Nave KA, Popko B. Myelination in the absence of galactolipids and proteolipid proteins. Mol Cell Neurosci. 1999;14:41-51.
- Coggan JS, Bittner S, Stiefel KM, Meuth SG, Prescott SA. Physiological Dynamics in Demyelinating Diseases: Unraveling Complex Relationships through Computer Modeling. Int J Mol Sci. 2015;16:21215-21236.

- Colakoglu G, Bergstrom-Tyrberg U, Berglund EO, Ranscht B. Contactin-1 regulates myelination and nodal/paranodal domain organization in the central nervous system. Proc Natl Acad Sci U S A. 2014;111:E394-403.
- Compston A, Coles A. Multiple sclerosis. Lancet. 2002;359:1221-1231.
- Davalos D, Grutzendler J, Yang G, et al. ATP mediates rapid microglial response to local brain injury in vivo. Nat Neurosci. 2005;8:752-758.
- Davies GR, Ramio-Torrenta L, Hadjiprocopis A, et al. Evidence for grey matter MTR abnormality in minimally disabled patients with early relapsing-remitting multiple sclerosis. J Neurol Neurosurg Psychiatry. 2004;75:998-1002.
- De Angelis DA, Braun PE. 2',3'-Cyclic nucleotide 3'-phosphodiesterase binds to actin-based cytoskeletal elements in an isoprenylation-independent manner. J Neurochem. 1996;67:943-951.
- De Stefano N, Matthews PM, Filippi M, et al. Evidence of early cortical atrophy in MS: relevance to white matter changes and disability. Neurology. 2003;60:1157-1162.
- Del Río Hortega P. (1920). Estudios sobre la neuroglía. La microglía y su transformación en células en bastoncito y cuerpos granuloadiposos. Trab. Lab. Invest. Biol. 18, 37–82.
- DeLuca GC, Ebers GC, Esiri MM. Axonal loss in multiple sclerosis: a pathological survey of the corticospinal and sensory tracts. Brain. 2004;127:1009-1018.

- DeVries G, Farrer R, Padadopoulos C, Campbell C, Litz J, Paletta, Dupree JL, Elford H. 2012. Didox-A Multipotent Drug for Treating Demyelinating disease. The FASEB Journal. 2012;26:341.4.
- Dupree JL, Coetzee T, Blight A, Suzuki K, Popko B. Myelin galactolipids are essential for proper node of Ranvier formation in the CNS. J Neurosci. 1998;18:1642-1649.
- Dupree JL, Mason JL, Marcus JR, et al. Oligodendrocytes assist in the maintenance of sodium channel clusters independent of the myelin sheath. Neuron Glia Biol. 2004;1:179-192.
- Dupree JL, Polak PE, Hensley K, Pelligrino D, Feinstein D. 2015 Beneficial effects of the CRMP-2 activator lanthionine ketimine ester in a mouse model of multiple sclerosis. J Neurochem 134(2):302-14.
- Dutta R, Trapp BD. Mechanisms of neuronal dysfunction and degeneration in multiple sclerosis. Prog Neurobiol. 2011;93:1-12.
- Dzhashiashvili Y, Zhang Y, Galinska J, Lam I, Grumet M, Salzer JL. Nodes of Ranvier and axon initial segments are ankyrin G-dependent domains that assemble by distinct mechanisms. J Cell Biol. 2007;177:857-870.
- Dzhashiashvili Y, Zhang Y, Galinska J, Lam I, Grumet M, Salzer JL. 2007. Nodes of Ranvier and axon initial segments are ankyrin G-dependent domains that assemble by distinct mechanisms. J Cell Biol 177:857-870.
- Edgar JM, McLaughlin M, Werner HB, et al. Early ultrastructural defects of axons and axon-glia junctions in mice lacking expression of Cnp1. Glia. 2009;57:1815-1824.

- Eisenbach M, Kartvelishvily E, Eshed-Eisenbach Y, et al. Differential clustering of Caspr by oligodendrocytes and Schwann cells. J Neurosci Res. 2009;87:3492-3501.
- Fabricius C, Berthold CH, Rydmark M. 1993. Axoplasmic organelles at nodes of Ranvier. II. Occurrence and distribution in large myelinated spinal cord axons of the adult cat. J Neurocytol 22:941-954.
- Ferguson B, Matyszak MK, Esiri MM, Perry VH. Axonal damage in acute multiple sclerosis lesions. Brain. 1997;120:393-399.
- Fields RD. Oligodendrocytes changing the rules: action potentials in glia and oligodendrocytes controlling action potentials. Neuroscientist. 2008;14:540-543.
- Files DK, Jausurawong T, Katrajian R, Danoff R. Multiple Sclerosis. *Primary Care: Clinics in Office Practice*. 2015;42:159-175.
- Fischer HG, Reichmann G. Brain dendritic cells and macrophages/microglia in central nervous system inflammation. J Immunol. 2001;166:2717-2726.
- Fisher E, Rudick RA, Cutter G, et al. Relationship between brain atrophy and disability: an 8-year follow-up study of multiple sclerosis patients. Mult Scler. 2000;6:373-377.
- Fraussen J, Claes N, de Bock L, Somers V. Targets of the humoral autoimmune response in multiple sclerosis. Autoimmun Rev. 2014;13:1126-1137.
- Frischer JM, Bramow S, Dal-Bianco A, et al. The relation between inflammation and neurodegeneration in multiple sclerosis brains. Brain. Oxford :2009;132:1175-1189.

- Funfschilling U, Supplie LM, Mahad D, et al. Glycolytic oligodendrocytes maintain myelin and long-term axonal integrity. Nature. 2012;485:517-521.
- Garbern JY, Yool DA, Moore GJ, et al. Patients lacking the major CNS myelin protein, proteolipid protein 1, develop length-dependent axonal degeneration in the absence of demyelination and inflammation. Brain. 2002;125:551-561.
- Gelman B. Diffuse microgliosis associated with cerebral atrophy in the acquired immunodeficiency syndrome. Annals of neurology. Boston] :1993;34:65-70.
- Ginhoux F, Greter M, Leboeuf M, et al. Fate mapping analysis reveals that adult microglia derive from primitive macrophages. Science. 2010;330:841-845.
- Gollan L, Salomon D, Salzer JL, Peles E. 2003. Caspr regulates the processing of contactin and inhibits its binding to neurofascin. J Cell Biol 163:1213-1218.
- Gomez-Nicola D, Fransen NL, Suzzi S, Perry VH. Regulation of microglial proliferation during chronic neurodegeneration. J Neurosci. 2013;33:2481-2493.
- Gonzalez-Scarano F, Baltuch G. Microglia as mediators of inflammatory and degenerative diseases. Annu Rev Neurosci. 1999;22:219-240.
- Greenfield JG. Demyelinating diseases. Greenfield's neuropathology /. London :2013:1513-1608.
- Griffiths I, Klugmann M, Anderson T, et al. Axonal swellings and degeneration in mice lacking the major proteolipid of myelin. Science. 1998;280:1610-

1613.

- Grigoriadis N, Ben-Hur T, Karussis D, Milonas I. Axonal damage in multiple sclerosis: a complex issue in a complex disease. *Clin Neurol Neurosurg*. 2004;106:211-217.
- Grimaud ,J., Barker G,J., Wang ,L., et al. Correlation of magnetic resonance imaging parameters with clinical disability in multiple sclerosis: a preliminary study. .
- Gusev E, Boiko A, Bikova O, et al. The natural history of early onset multiple sclerosis: comparison of data from Moscow and Vancouver. Clin Neurol Neurosurg. 2002;104:203-207.
- Haines JD, Inglese M, Casaccia P. Axonal Damage in Multiple Sclerosis. Mt Sinai J Med. 2011;78:231-243.
- Harbo H,F., Gold ,Ralf, TintorÃ© ,Mar. .
- Hartline DK, Colman DR. Rapid Conduction and the Evolution of Giant Axons and Myelinated Fibers. Current Biology. 2007;17:R29-R35.
- Hauser SL, Oksenberg JR. The neurobiology of multiple sclerosis: genes, inflammation, and neurodegeneration. Neuron. 2006;52:61-76.
- He M, Tseng WC, Bennett V. A single divergent exon inhibits ankyrin-B association with the plasma membrane. J Biol Chem. 2013;288:14769-14779.
- Hedstrom KL, Ogawa Y, Rasband MN. AnkyrinG is required for maintenance of the axon initial segment and neuronal polarity. J Cell Biol. 2008;183:635-640.
- Hickman S,E., Kingery N,D., Ohsumi T,K., et al. The microglial sensome

revealed by direct RNA sequencing. .

- Hiremath MM, Saito Y, Knapp GW, Ting JP, Suzuki K, Matsushima GK. 1998. Microglial/macrophage accumulation during cuprizone-induced demyelination in C57BL/6 mice. J Neuroimmunol 92:38-49.
- Hutson CB, Lazo CR, Mortazavi F, Giza CC, Hovda D, Chesselet MF. Traumatic brain injury in adult rats causes progressive nigrostriatal dopaminergic cell loss and enhanced vulnerability to the pesticide paraquat. J Neurotrauma. 2011;28:1783-1801.
- Irvine KA, Blakemore WF. Remyelination protects axons from demyelination-associated axon degeneration. Brain. 2008;131:1464-1477.
- Jahn O, Tenzer S, Werner HB. Myelin proteomics: molecular anatomy of an insulating sheath. Mol Neurobiol. 2009;40:55-72.
- Jeffery ND, Blakemore WF. Locomotor deficits induced by experimental spinal cord demyelination are abolished by spontaneous remyelination. Brain. 1997;120:27-37.
- Jenkins SM, Bennett V. Developing nodes of Ranvier are defined by ankyrin-G clustering and are independent of paranodal axoglial adhesion. Proceedings of the National Academy of Sciences. 2002;99:2303-2308.
- Kettenmann H, Hanisch UK, Noda M, Verkhratsky A. Physiology of microglia. Physiol Rev. 2011;91:461-553.
- Khan M, Singh J, Singh I. Plasmalogen deficiency in cerebral adrenoleukodystrophy and its modulation by lovastatin. J Neurochem. 2008;106:1766-1779.

- Kim JK, Mastronardi FG, Wood DD, Lubman DM, Zand R, Moscarello MA. Multiple sclerosis: an important role for post-translational modifications of myelin basic protein in pathogenesis. Mol Cell Proteomics. 2003;2:453-462.
- Klugmann M, Schwab MH, Puhlhofer A, et al. Assembly of CNS myelin in the absence of proteolipid protein. Neuron. 1997;18:59-70.
- Kole MP, Stuart G. Signal Processing in the Axon Initial Segment. Neuron. 2012;73:235-247.
- Komada M, Soriano P. 2002. Beta IV-spectrin regulates sodium channel clustering through ankyrin-G at axon initial segments and nodes of Ranvier. J Cell Biol 156:337- 348.
- Kordeli E, Lambert S, Bennett V. AnkyrinG. A new ankyrin gene with neural-specific isoforms localized at the axonal initial segment and node of Ranvier. J Biol Chem. 1995;270:2352-2359.
- Kornek B, Lassmann H. Axonal pathology in multiple sclerosis. A historical note. Brain Pathol. 1999;9:651-656.
- Kornek B, Storch MK, Weissert R, et al. Multiple sclerosis and chronic autoimmune encephalomyelitis: a comparative quantitative study of axonal injury in active, inactive, and remyelinated lesions. Am J Pathol. 2000;157:267-276.
- Kutzelnigg A, Lassmann H. Pathology of multiple sclerosis and related inflammatory demyelinating diseases. Handb Clin Neurol. 2014;122:15-58.
- Lee SC, Liu W, Dickson DW, Brosnan CF, Berman JW. Cytokine production by human fetal microglia and astrocytes. Differential induction by

lipopolysaccharide and IL-1 beta. The Journal of Immunology. 1993;150:2659-2667.

- Lee Y, Morrison BM, Li Y, et al. Oligodendroglia metabolically support axons and contribute to neurodegeneration. Nature. 2012;487:443-448.
- Levin MC, Lee S, Gardner LA, Shin Y, Douglas JN, Cooper C. Autoantibodies to Non-myelin Antigens as Contributors to the Pathogenesis of Multiple Sclerosis. J Clin Cell Immunol. 2013;4:10.4172/2155-9899.1000148.
- Li C, Tropak MB, Gerlai R, et al. Myelination in the absence of myelin-associated glycoprotein. Nature. 1994;369:747-750.
- Li H, Cuzner ML, Newcombe J. Microglia-derived macrophages in early multiple sclerosis plaques. Neuropathol Appl Neurobiol. 1996;22:207-215.
- Ling E, Wong W. The origin and nature of ramified and amoeboid microglia: A historical review and current concepts. Glia. 1993;7:9-18.
- Loane DJ, Kumar A. Microglia in the TBI brain: The good, the bad, and the dysregulated. Exp Neurol.
- Lovas G, Szilágyi N, Majtényi K, Palkovits M, Komoly S. Axonal changes in chronic demyelinated cervical spinal cord plaques. Brain. 2000;123:308-317.
- Lu J, Moochhala S, Kaur C, Ling EA. Cellular inflammatory response associated with breakdown of the blood-brain barrier after closed head injury in rats. J Neurotrauma. 2001;18:399-408.
- Lublin FD, Reingold SC, Cohen JA, et al. Defining the clinical course of multiple sclerosis: the 2013 revisions. Neurology. 2014;83:278-286.
- Lucchinetti C, Bruck W. The pathology of primary progressive multiple

sclerosis. Multiple Sclerosis. Houndmills, Basingstoke, Hampshire, UK] :2004;10:23-30.

- Mahad DH, Trapp BD, Lassmann H. Pathological mechanisms in progressive multiple sclerosis. The Lancet Neurology. 2015;14:183-193.
- Mason JL, Langaman C, Morell P, Suzuki K, Matsushima GK. 2001. Episodic demyelination and subsequent remyelination within the murine central nervous system; changes in axonal caliber. Neuropathology and Applied Neurobiology 27:50-58.
- Mathews ES, Mawdsley DJ, Walker M, Hines JH, Pozzoli M, Appel B. Mutation of 3-Hydroxy-3-Methylglutaryl CoA Synthase I Reveals Requirements for Isoprenoid and Cholesterol Synthesis in Oligodendrocyte Migration Arrest, Axon Wrapping, and Myelin Gene Expression. The journal of neuroscience. Washington, D.C. :2014;34:3402-3412.
- Matsushima GK and Morell P. 2001. The neurotoxicant, cuprizone as a model to study demyelination and remyelination in the central nervous system. Brain Pathol 11(1):107-16.
- Matthews P, De Stefano N, Narayanan S, et al. Putting Magnetic Resonance Spectroscopy Studies in Context: Axonal Damage and Disability in Multiple Sclerosis. Seminars in neurology. New York, NY :1998;18:327-336.
- McGeer PL, Kawamata T, Walker DG, Akiyama H, Tooyama I, McGeer EG. Microglia in degenerative neurological disease. Glia. 1993;7:84-92.
- Mews I, Bergmann M, Bunkowski S, Gullotta F, Bruck W. Oligodendrocyte and axon pathology in clinically silent multiple sclerosis lesions. Mult Scler.

1998;4:55-62.

- Miller DH, Barkhof F, Frank JA, Parker GJ, Thompson AJ. Measurement of atrophy in multiple sclerosis: pathological basis, methodological aspects and clinical relevance. Brain. 2002;125:1676-1695.
- Miller DH, Chard DT, Ciccarelli O. Clinically isolated syndromes. Lancet Neurol. 2012;11:157-169.
- Morell P, Quarles R. Characteristic composition of myelin. in: . In: Siegel G, Agranoff B, Albers R, eds. Basic Neurochemistry: Molecular, Cellular and Medical Aspects. 6th Edition. Philadelphia: Lippincott-Raven; 1999. Available from: Http://www.Ncbi.Nlm.Nih.gov/books/NBK28221/. ; 1999.
- Nave KA, Werner HB. Myelination of the nervous system: mechanisms and functions. Annu Rev Cell Dev Biol. 2014;30:503-533.
- Neumann H, Boucraut J, Hahnel C, Misgeld T, Wekerle H. Neuronal control of MHC class II inducibility in rat astrocytes and microglia. Eur J Neurosci. 1996;8:2582-2590.
- Nimmerjahn A, Kirchhoff F, Helmchen F. Resting microglial cells are highly dynamic surveillants of brain parenchyma in vivo. Science. 2005;308:1314-1318.
- Noseworthy JH, Lucchinetti C, Rodriguez M, Weinshenker BG. Multiple Sclerosis. N Engl J Med. 2000;343:938-952.
- Noseworthy JH. Progress in determining the causes and treatment of multiple sclerosis. Nature. 1999;399:A40-7.
- O'Connor K,C., McLaughlin K,A., De Jager P,L., et al. Self-antigen tetramers

discriminate between myelin autoantibodies to native or denatured protein. .

- O'Connor LT, Goetz BD, Kwiecien JM, Delaney KH, Fletch AL, Duncan ID. Insertion of a retrotransposon in Mbp disrupts mRNA splicing and myelination in a new mutant rat. J Neurosci. 1999;19:3404-3413.
- Ogawa Y, Rasband MN. The functional organization and assembly of the axon initial segment. Curr Opin Neurobiol. 2008;18:307-313.
- Olson JK, Miller SD. Microglia Initiate Central Nervous System Innate and Adaptive Immune Responses through Multiple TLRs. The Journal of Immunology. 2004;173:3916-3924.
- Oluich LJ, Stratton JA, Xing YL, et al. Targeted ablation of oligodendrocytes induces axonal pathology independent of overt demyelination. J Neurosci. 2012;32:8317-8330.
- Orton SM, Ramagopalan SV, Brocklebank D, et al. Effect of immigration on multiple sclerosis sex ratio in Canada: the Canadian Collaborative Study. J Neurol Neurosurg Psychiatry. 2010;81:31-36.
- Paolillo A, Pozzilli C, Gasperini C, et al. Brain atrophy in relapsing-remitting multiple sclerosis: relationship with 'black holes', disease duration and clinical disability. J Neurol Sci. 2000;174:85-91.
- Perez-Cerda F, Sanchez-Gomez MV, Matute C. Pio del Rio Hortega and the discovery of the oligodendrocytes. Front Neuroanat. 2015;9:92.
- Peters A, Palay S L & Webster H deF. The fine structure of the nervous system. The neurons and supporting cells. New York: Harper and Row, 1970.

198 p.; and The fine structure of the nervous system. The neurons and supporting cells. Philadelphia: Saunders, 1976. 406 p.

- Popescu BF, Lucchinetti CF. Pathology of demyelinating diseases. Annu Rev Pathol. 2012;7:185-217.
- Prineas JW, Kwon EE, Cho E, et al. Immunopathology of secondary-progressive multiple sclerosis. Annals of neurology. Boston] :2001;50:646-657.
- Prinz M, Priller J. Microglia and brain macrophages in the molecular age: from origin to neuropsychiatric disease. Nat Rev Neurosci. 2014;15:300-312.
- Ramio-Torrenta L, Sastre-Garriga J, Ingle GT, et al. Abnormalities in normal appearing tissues in early primary progressive multiple sclerosis and their relation to disability: a tissue specific magnetisation transfer study. J Neurol Neurosurg Psychiatry. 2006;77:40-45.
- Ransohoff RM, Perry VH. Microglial physiology: unique stimuli, specialized responses. Annu Rev Immunol. 2009;27:119-145.
- RaymondA S, GRWayne M. Demyelinating diseases. .
- Reeves TM, Greer JE, Vanderveer AS, Phillips LL. Proteolysis of submembrane cytoskeletal proteins ankyrin-G and alphaII-spectrin following diffuse brain injury: a role in white matter vulnerability at Nodes of Ranvier. Brain Pathol. 2010;20:1055-1068.
- Renoux C, Vukusic S, Mikaeloff Y, et al. Natural history of multiple sclerosis with childhood onset. N Engl J Med. 2007;356:2603-2613.
- Roach A, Takahashi N, Pravtcheva D, Ruddle F, Hood L. Chromosomal

mapping of mouse myelin basic protein gene and structure and transcription of the partially deleted gene in shiverer mutant mice. Cell. 1985;42:149-155.

- Rudick RA, Fisher E, Lee JC, Simon J, Jacobs L. Use of the brain parenchymal fraction to measure whole brain atrophy in relapsing-remitting MS. Multiple Sclerosis Collaborative Research Group. Neurology. 1999;53:1698-1704.
- Saaltink D, Håvik B, Verissimo CS, Lucassen PJ, Vreugdenhil E. Doublecortin and doublecortin-like are expressed in overlapping and non-overlapping neuronal cell population: Implications for neurogenesis. J Comp Neurol. 2012;520:2805-2823.
- Saher G, Quintes S, Mobius W, et al. Cholesterol Regulates the Endoplasmic Reticulum Exit of the Major Membrane Protein P0 Required for Peripheral Myelin Compaction. The journal of neuroscience. Washington, D.C. :2009;29:6094-6104.
- Saher G. High cholesterol level is essential for myelin membrane growth. Nature neuroscience. New York, N.Y. :2005;8:468.
- Salzer JL. 1997. Clustering sodium channels at the node of Ranvier: close encounters of the axon-glia kind. Neuron 18:843-846.
- Schafer DP, Jha S, Liu F, Akella T, McCullough LD, Rasband MN. Disruption of the axon initial segment cytoskeleton is a new mechanism for neuronal injury. J Neurosci. 2009;29:13242-13254.
- Schafer DP, Lehrman EK, Kautzman AG, et al. Microglia sculpt postnatal neural circuits in an activity and complement-dependent manner. Neuron. 2012;74:691-705.

- Secor McVoy JR, Oughli HA, Oh U. 2015. Liver X receptor-dependent inhibition of microglial nitric oxide synthase 2. Journal of Neuroinflammation 12:27.
- Shemer A, Erny D, Jung S, Prinz M. Microglia Plasticity During Health and Disease: An Immunological Perspective. Trends Immunol. 2015;36:614-624.
- Sherman DL, Tait S, Melrose S, Johnson R, Zonta B, Court FA, Macklin WB, Meek S, Smith AJ, Cottrell DF, Brophy PJ. 2005. Neurofascins are required to establish axonal domains for saltatory conduction. Neuron 48:737-742.
- Siffrin V, Vogt J, Radbruch H, Nitsch R, Zipp F. Multiple sclerosis - candidate mechanisms underlying CNS atrophy. Trends Neurosci. 2010;33:202-210.
- Simone IL, Carrara D, Tortorella C, et al. Course and prognosis in early-onset MS: comparison with adult-onset forms. Neurology. 2002;59:1922-1928.
- Skripuletz T, Lindner M, Kotsiari A, Garde N, Fokuhl J, Linsmeier F, Trebst C, Stangel M. 2008. Cortical demyelination is prominent in the murine cuprizone model and is strain- dependent. Am J Path 172(4):1053-1061.
- Slavik JM, Hutchcroft JE, Bierer BE. CD28/CTLA-4 and CD80/CD86 families: signaling and function. Immunol Res. 1999;19:1-24.
- Smith KJ. Nitric Oxide and Axonal Pathophysiology. 2005:255-273.
- Smolders J, Schuurman KG, van Strien ME, et al. Expression of vitamin D receptor and metabolizing enzymes in multiple sclerosis-affected brain tissue. J Neuropathol Exp Neurol. 2013;72:91-105.
- Snaidero N, Simons M. Myelination at a glance. J Cell Sci. 2014;127:2999-3004.

- Sobotzik J, Sie JM, Politi C, et al. AnkyrinG is required to maintain axo-dendritic polarity in vivo. Proceedings of the National Academy of Sciences. 2009;106:17564-17569.
- Stiess M, Bradke F. Neuronal polarization: The cytoskeleton leads the way. Developmental Neurobiology. 2011;71:430-444.
- Susuki K, Rasband MN. Molecular mechanisms of node of Ranvier formation. Curr Opin Cell Biol. 2008;20:616-623.
- Taetzsch T, Levesque S, McGraw C, et al. Redox regulation of NF-?B p50 and M1 polarization in microglia. Glia. 2015;63:423-440.
- Thaxton C, Bhat MA. 2009. Myelination and regional domain differentiation of the axon. Results Probl Cell Differ 48:1-28.
- Tomassy GS, Dershowitz LB, Arlotta P. Diversity Matters: A Revised Guide to Myelination. Trends Cell Biol. 2015.
- Tonra JR, Reiseter BS, Kolbeck R, et al. Comparison of the timing of acute blood-brain barrier breakdown to rabbit immunoglobulin G in the cerebellum and spinal cord of mice with experimental autoimmune encephalomyelitis. J Comp Neurol. 2001;430:131-144.
- Trapp BD, Nave KA. Multiple sclerosis: an immune or neurodegenerative disorder? Annu Rev Neurosci. 2008;31:247-269.
- Trapp BD, Peterson J, Ransohoff RM, Rudick R, Mörk S, Bö L. Axonal Transection in the Lesions of Multiple Sclerosis. N Engl J Med. 1998;338:278-285.
- Tremblay ME, Lecours C, Samson L, Sanchez-Zafra V, Sierra A. From the Cajal

alumni Achucarro and Rio-Hortega to the rediscovery of never-resting microglia. Front Neuroanat. 2015;9:45.

- Tremlett H, Paty D, Devonshire V. Disability progression in multiple sclerosis is slower than previously reported. Neurology. 2006;66:172-177.
- Vanderlugt CL, Miller SD. Epitope spreading in immune-mediated diseases: implications for immunotherapy. Nat Rev Immunol. 2002;2:85-95.
- von Herrath MG, Fujinami RS, Whitton JL. Microorganisms and autoimmunity: making the barren field fertile? Nat Rev Microbiol. 2003;1:151-157.
- Waisman A, Ginhoux F, Greter M, Bruttger J. Homeostasis of Microglia in the Adult Brain: Review of Novel Microglia Depletion Systems. Trends Immunol. 2015;36:625-636.
- Wallin MT, Culpepper WJ, Coffman P, et al. The Gulf War era multiple sclerosis cohort: age and incidence rates by race, sex and service. Brain. 2012;135:1778-1785.
- Wefelmeyer ,Winnie, Cattaert ,Daniel, Burrone ,Juan. Activity-dependent mismatch between axo-axonic synapses and the axon initial segment controls neuronal output. . 2015.
- Wingerchuk DM, Weinshenker BG. The natural history of multiple sclerosis: implications for trial design. Curr Opin Neurol. 1999;12:345-349.
- Yim SH, Quarles RH. Biosynthesis and expression of the myelin-associated glycoprotein in cultured oligodendrocytes from adult bovine brain. J Neurosci Res. 1992;33:370-378.

- Yoshimura T, Rasband MN. Axon initial segments: diverse and dynamic neuronal compartments. Curr Opin Neurobiol. 2014;27:96-102.
- Zhang Y, Da R, Hilgenberg LG, et al. Clonal expansion of IgA-positive plasma cells and axon-reactive antibodies in MS lesions. J Neuroimmunol. 2005;167:120-130.
- Zhou D, Lambert S, Malen PL, Carpenter S, Boland LM, Bennett V. AnkyrinG is required for clustering of voltage-gated Na channels at axon initial segments and for normal action potential firing. J Cell Biol. 1998;143:1295-1304.

VITA

Suneel Krishna Thummala was born in Bangalore, Karnataka, India, on April 9, 1987. He graduated with a Bachelor of Medicine, Bachelor of Surgery (M.B.B.S.) from Vydehi Institute of Medical Sciences and Research Centre, Bangalore, KA. He currently resides in Richmond, Virginia.